ANALYSIS OF ABORAL SPINE VARIATION IN THE FORCIPULATE SEA STAR, *PISASTER OCHRACEUS* (BRANDT 1835)

By

Angela Jordane Jones

A Thesis Presented to

The Faculty of Humboldt State University

In Partial Fulfillment of the Requirements for the Degree

Master of Science in Biology

Committee Membership

Dr. Paul Bourdeau, Committee Chair

Dr. Edward Metz, Committee Member

Dr. John Reiss, Committee Member

Dr. Brian Tissot, Committee Member

Dr. Erik Jules, Program Graduate Coordinator

May 2019

ABSTRACT

ANALYSIS OF ABORAL SPINE VARIATION IN THE FORCIPULATE SEA STAR, *PISASTER OCHRACEUS* (BRANDT 1835)

Angela Jordane Jones

Rocky intertidal zones are highly dynamic environments that exhibit substantial spatial and temporal variation in abiotic conditions, which can drive body form variation and energy allocation within calcifying species. Wave exposure, specifically, has been shown to be a significant driver of skeletal and structural morphology in organisms including gastropods, bivalves, and sponges. Many of such organisms, from sponges to echinoderms, rely on calcium carbonate for structural support and protection.

In the phylum Echinodermata (named for possessing a 'spiny skin'), research on the form and function of calcium carbonate spines is largely relegated to Class Echinodea (e.g., urchins and sand dollars) and superorders Spinulosacea and Valvatacea within Class Asteroidea (sea stars). Few studies have provided morphological descriptions and functional hypotheses for spines in the Superorder Forcipulatida within Asteroidea. Here, I examine aboral spine morphology and variation in the forcipulate seastar, *Pisaster ochraceus*, a habitat generalist in rocky intertidal zones of the eastern North Pacific. I found that aboral spine density was significantly higher in sea stars in more physically-harsh bench and boulder field habitats compared to more physically-benign habitats like protected embayments. I also found specific aboral spine morphotypes that were

associated with specific habitats; sea stars in protected embayments had spines that were upright and columnar, whereas bench and boulder field sea stars had shorter, convex spines. I hypothesize that dense, convex aboral spines have the potential to function as protection for the aboral surface of sea stars in habitats exposed to the combined stresses of high wave action and sediment load, but future studies are necessary to fully elucidate function.

ACKNOWLEDGEMENTS

I would like to start by thanking my advisor Dr. Paul Bourdeau. I joined his lab in 2015 and his mentorship over the past four years has been instrumental in bettering my love of academia. His attention to detail and willingness to try new things have made it possible for me to explore countless avenues for this project. I will always be grateful. I would like to my committee for the valuable input that they gave me. Dr. Ed Metz provided valuable insight with echinoderm development, Dr. John Reiss for his knowledge in morphology, and Dr. Brian Tissot for his experience in intertidal ecology and *Pisaster ochraceus.*

I am also thankful for the PEB lab: Tayler Tharaldson, Tharadet Man, Timothy McClure, Wesley Hull, Lily McIntire, Kindall Murie, Andrea Fiber, and Jessica Gravel. I could not have done this without my team of volunteers. My lead assistant, Angelina Zuelow, was instrumental in this project. My team also included Kyle Orr, Carrissa Hernandez, Ashland Aguilar, Emily Nielsen, Ethan Abercrombie, Raili Makela, Kristofer Bauer, Barbara Orozco, and Heidi Sanders.

Thank you to all the faculty and staff that have assisted me in equipment training and use of supplies: Dave Baston in the Core Facility, Susan Wright in the stockroom, Marty Reed with electron microscopy, Casey Lu and John Reiss for training in Scanning Electron Microscopy, and Allison Bronson who helped me with Mimics Software for 3D printing.

I would also like to thank Point Defiance Zoo and Aquarium and the Animal Welfare Committee for allowing me to examine sea stars from the aquarium. The staff at PDZA was very helpful including my point of contact, Melissa Bishop, an aquarist. Lastly, I would also like to thank Seth Hogg and Rajaram Manoharan who assisted me with MicroCT Scans from Micro Photonics Inc. The time and effort that they have put in was invaluable.

I would also like to thank all of the funding sources that helped me with travel and supplies for my thesis: Humboldt Marine and Coastal Science Institute (HMCSI) and the Malcolm Oliphant Scholarship.

TABLE OF CONTENTS

LIST OF TABLES

LIST OF FIGURES

LIST OF APPENDICES

INTRODUCTION

The rocky intertidal zone has been described as one of the most stressful environments on earth because of its multitude of biotic and abiotic stressors (Helmuth and Denny, 2003; Menge, 1976). 'Intertidal' is an umbrella term, however, used to describe the space between terrestrial lands and subtidal waters that encompasses many habitat types (Ricketts *et al.,* 1968). These habitats include cobble fields, boulder fields, expansive rock benches, island ridges, sandy beaches, and mudflats. Each of these habitats vary with respect to the frequency and intensity of physical stressors, including thermal fluctuations, sediment accretion, and hydrodynamic forces (e.g., waves and currents) (Ricketts *et al.,* 1968; Denny, 1991; Sanford, 2002).

One of the most prominent stressors that intertidal organisms are exposed to and varies across these habitats are wave forces (Denny and Helmuth, 2003). Different intertidal habitats can vary in exposure to both wave intensity and frequency (Gaylord, 2000; 2007), and this has consequences for organismal fitness. In higher wave-exposed habitats, dislodgment risk for organisms in the intertidal increases exponentially due to the increase of drag and lift forces acting on the organism (Denny, 2014). However, dislodgment is not the only potential risk. Structural damage to organisms and even death can occur in the intertidal zone due to forces associated with wave shock (Denny and Helmuth, 2003), and in some habitats the combination of high sediment load and hydrodynamic forces can cause abrasion to, and particle settlement on, soft tissue surfaces, causing damage and limiting respiration (Mooi, 1986).

Wave intensity in the intertidal zone can be a substantial selective force on echinoderms, and as such, many species exhibit habitat-specific variability in traits that protect them against hydrodynamic stressors. For example, purple sea urchins (*Strongylocentrotus purpuratus*) in wave-exposed habitats often exhibit reduced size to reduce risk of destruction by waves (Denny *et al.,* 1985) and can streamline their autonomous aboral spines downward to reduce drag and lift forces in response to high water flow (George and Carrington, 2014). Other urchin species reduce tube foot adhesive compounds when moved from field conditions to laboratory settings, suggesting high energetic costs and adaptive value for increased tube foot adhesion in wave-exposed conditions (Toubarro *et al.*, 2016). Whereas all of these examples come from sea urchins, it is reasonable to predict that other intertidal groups of echinoderms should exhibit habitat-specific variability in traits that defend them against hydrodynamic stress.

The ochre sea star (*Pisaster ochraceus*) inhabits a wide variety of habitats, including wave-protected bays and subtidal habitats, and more wave-exposed intertidal habitats such as boulder fields, benches, and human-made jetties. Previous studies have shown that *P. ochraceus* exhibits adaptive variation in traits that protect it from wave-related stress. For example, individuals in high wave action environments have stronger tube feet than those in wave protected habitats, and after transplant from a benign wave environment to a higher wave action location, adhesive strength of the tube feet increases (Hayne, 2011). *P. ochraceus* can also plastically alter its body shape to reduce drag and lift forces; with individuals in wave-exposed habitats becoming flatter and thinner than those individuals in wave-protected habitats, and once moved to a protected environment

increased arm width and body height (Hayne and Palmer, 2013). Further, previous authors have noted that *P. ochraceus* in calm or benign hydrodynamic environments appear as an 'inflated' morph with a high proportion of soft tissue and wide rays, while those in environments with higher wave forces appear 'spinier' with a 'starved' appearance with a heavily ossified aboral surface and low proportion of soft tissue (Feder, 1970). Hayne and Palmer (2013) also observed, but did not quantify, the presence of *P. ochraceus* with spinier body forms residing in more wave-exposed habitats. Thus, previous work suggests that aboral spines may be more prevalent in *P. ochraceus* residing in more wave-exposed habitats, but this association has not been examined quantitatively.

Endo-skeletal elements are not often the primary focus of descriptive studies of anatomical variation in asteroids, with aboral spines often mentioned as an afterthought and sometimes referred to as "associated appendages" (Blowes *et al.*, 2017; Elyers, 1976). Thus, we currently know very little about the variation in form and function of aboral spines in asteroids, with some notable exceptions. For example, asteroids in the superorders Spinulosacea and Valvatacea, referred to as "the heavily armored sea stars", display notable interspecific similarities and differences with the possession of large ossicles and wide polygonal spines that protect vulnerable areas on the both the oral and aboral surfaces (Blake, 1983). In the superorder Forcipulatida, inter- and intraspecific variation in aboral spines have not been well studied. Fisher (1930) illustrated numerous spines in northeastern Pacific species in this group, including *Pisaster* and *Leptasterias* spp., both of which showed obvious spine size and shape variation, but this variation was

not formally described. Later, Leclair (1993) described different spine shapes in *Pisaster* spp., documenting differences in both spine width and height, and describing ochre sea star (*P. ochraceus)*, spines as mushroom or knob-shaped, with thickened ridges on the top of the spine that appear to be in line with Fisher's illustrations. As such, *P. ochraceus* is potentially a good model for studying intraspecific variation in form and function of asteroid aboral spine morphology. *P. ochraceus* is abundant in the rocky intertidal zone from Alaska to Baja, California (Paine, 1969), exhibits marked morphological variability in several traits (e.g., color; Ramundi *et al.*, 2007), and has been previously hypothesized to be a complex of subspecies due to variation in spine coverage on its aboral surface (Feder, 1970; see Figure 1). Fisher (1930) suggested four morphologically distinct subspecies of *P. ochraceus* based in part on variation in aboral spine patterning and size. The subspecies designations were later rejected due to genetic homogeneity across its distribution with the consensus that *P. ochraceus* is, instead, recognized as a single species (Frontana-Uribe *et al.*, 2008). However, the original characterization of subspecies suggests high levels of intraspecific variation in aboral spines.

In my thesis, I characterize and quantify intraspecific variation in *P. ochraceus* aboral spines, including ontogenetic and spatial variation in shape, size, and density (number of spines per unit area on the aboral surface). I also classify a unique set of spine categories and provide descriptions of spine microstructural anatomy. Specifically, I will examine (1) relationships between aboral spine variation across a range of rocky intertidal habitats, and (2) associations between aboral spine variation and other traits

associated with resistance to wave exposure, to assess the potential functional and adaptive significance of intraspecific aboral spine variation in *P. ochraceus*.

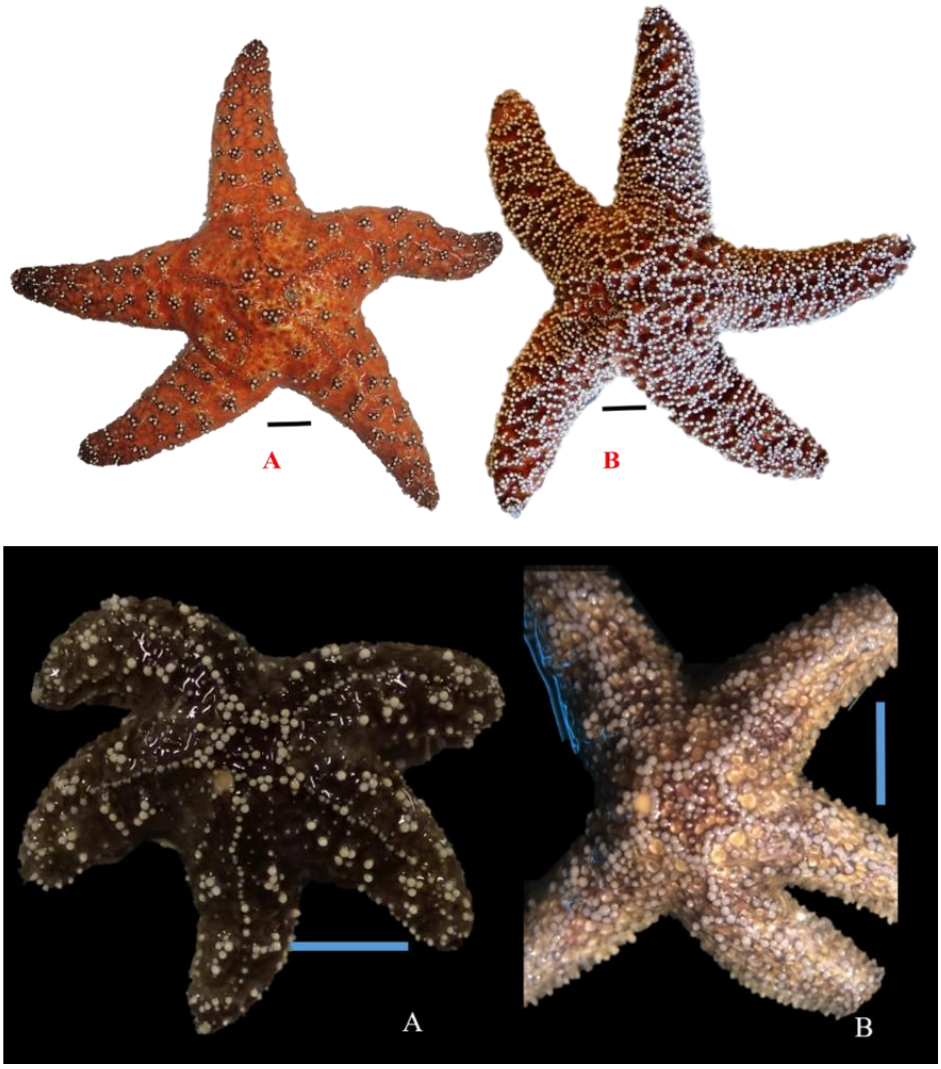

Figure 1. Planar view of *Pisaster ochraceus* showing representative intraspecific variation in aboral spines of adult (top) and juvenile (bottom) sea stars (scale bar is 10 mm). Individuals from bays (A) contain few spines and more visible soft tissue; individuals from boulder fields (B) have high aboral spine coverage and little visible soft tissue.

METHODS

Site Locations and Collection Protocols

I examined three intertidal habitat types – boulder fields, rock benches, and protected embayments (Figure 2 and Table 1) – where *Pisaster ochraceus* is found. The boulder field habitats were Point St George (PSG), False Klamath Cove (FKC), and Baker Beach (BB). These boulder fields are made up variably sized rock, including cobble and sand, but are dominated by large boulders. Bench survey sites were Strawberry Hill (SH), Kibesillah Hill (KH), and Noyo Headlands (NH), which are large expanses of continuous bedrock, dominated by *Mytilus californianus* beds and surrounded by surge channels (Strawberry Hill: Menge 1992). I used two locations in Humboldt Bay as protected embayment sites: King Salmon (KS) and Del Norte Dock (DND). KS is a human-made jetty comprised of an assemblage of large rocks that function as a protective bank between the entrance channel to the bay, and surrounding waterfront neighborhoods, while DND consists of large cement pillars embedded in a mud bottom. I also collected adult sea stars from the Point Defiance Zoo and Aquarium (PDZA), which served as a benign habitat 'control.' The sea stars that reside at PDZA live in a deep, calm-water two-story tank with numerous subtidal species cohabitating a low stress environment.

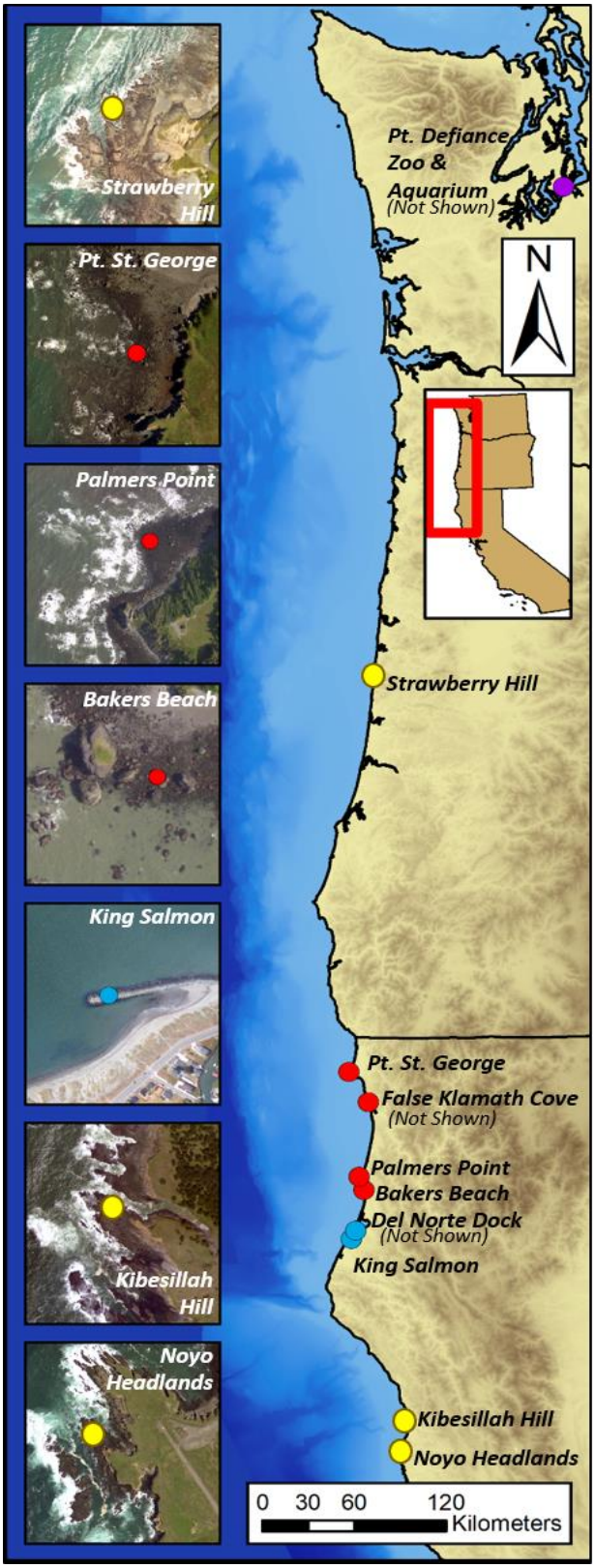

Figure 2. Map of all source locations. PDZA = Point Defiance Zoo and Aquarium, SH = Strawberry Hill, PSG = Point St George, FKC = False Klamath Cove, PP = Palmer's Point, BB = Baker Beach, DND = Del Norte Dock, KS = King Salmon, KH = Kibesillah Hill, and NH = Noyo Headlands. Color points represent habitat types: Purple is the benign control PDZA, yellow is rock bench habitat (SH, KH, and NH), red is boulder field habitat (PSG, FKC, PP, and BB), and blue is bay habitat (KS and DND).

Table 1. Sampling locations, habitat types, and times.

Collection Site	Code	Coordinates	Habitat Type	Site Characteristic Data	Continuous Sampling? Y/N	Years Sampled
Point Defiance Zoo and Aquarium	PDZA	47°18’24”N 122°30’56”W	Benign (Control)	N	N	2016
Strawberry Hill	SH	44.25°N, 124.11°W	Bench	N	N	2018
Point St George	PSG	41.783°N, 124.256°W	Boulder Field	Y	Y	2015-2017
False Klamath Cove	FKC	41.593°N, 124.107°W	Boulder Field	N	N	2015-2017
Palmer's Point	PP	41.132°N, 124.164°W	Boulder Field	N	N	2015-2017
Baker Beach	BB	41.044°N, 124.123°W	Boulder Field	Y	Y	2015-2017
Del Norte Dock	DND	40.790°N, 124.188°W	Bay	N	N	2017-2018
King Salmon	KS	40.743°N, 124.216°W	Bay	Y	N	2017
Kibesillah Hill	KH	39.588°N, 123.782°W	Bench	Y	Y	2015-2017
Noyo Headlands	NH	39.437°N, 123.819°W	Bench	Y	Y	2015-2017

To characterize and quantify variation in aboral spine density, size, and morphology, I collected 25 to 40 individual *P. ochraceus* from the intertidal zone at eight locations in Northern California and Oregon in summer and winter seasons between 2015 and 2018 (Fig 2). I also measured adult sea stars from the PDZA in Pierce County, WA in 2016. I recorded measurements of sea stars from PDZA using digital calipers for the following: sea star radius (Euclidean distance from the center of the central disc to the distal end of the longest ray), central disc height and width, and ray width. I also performed aboral spine removal on site with the approval of the PDZA Animal Welfare Committee. Sea stars from Strawberry Hill (Oregon) were measured in the same way as the sea stars at PDZA, without removing sea stars from the site. For collection sites in California, I brought the collected sea stars to the Telonicher Marine Lab (TML) in Trinidad, CA for the aforementioned measurements and aboral spine removal. I returned the sea stars to their collection locations within 48 h. While at TML, I captured planar-view images of each sea star with a digital camera (Olympus TG-3 Waterproof 16 MP Digital Camera) fastened to a copy stand at a standardized distance of 28 cm from the aboral surface of the sea star. Fifteen aboral spines, referred to as primary spines (as they were the largest), were haphazardly removed from central and peripheral regions of the aboral surface of ten sea stars from each sampling site, using fine forceps under light microscopy.

Prior to the start of this study, I performed the spine removal protocols on stars held in the TML in running sea water. Over the course of two months, I did not find any of the following: reduction in feeding, abnormal behavior, sudden wasting symptoms,

physical damage, or death. In my experience, aboral spine removal is mild and not likely to cause significant harm to the sea star.

Aboral Spine Density

I used digital photographs to quantify spine variation on the aboral surface of the central disc of each sea star. All digital photographs of sea stars were pre-processed for particle counting and area measurements of complex object optimization in Software ImageJ (Schneider *et al.*, 2012). This allowed me to isolate the image of the central disc, reduce the image type from RBG to 8-bit, and render the photo to black and white (see Figure 3 A and B), which reduced any small particle interference from the rest of the image. From these images I obtained the number and area of every spine on the aboral surface of each sea star with added batch programs in ImageJ (AutoTheshold, Convert to Mask, Erode, Dilate, Watershed, and Analyze Particles) to reinforce spine outlines and to reduce watermarks from the soft tissue as seen in Figure 3C. I used the output from ImageJ and divided the total number of spines counted by the total area of the central disc to obtain spine density (no. spines $\cdot$ mm^{-2}) for each individual sea star. I used particle area in the batch programs to calculate spine area for each individual spine. Spine area was averaged across all spines for each sea star. Fourteen individuals were used to examine the relationship between central disc aboral spine density and whole sea star aboral spine density. I did this to ensure that the central disc provides accurate representation of whole sea star spine load, because the isolation of the central disc is more efficient than using

the whole sea star. Photographs were pre-processed to obtain two images of each sea star: an isolated central disc and a whole sea star with all background removed. I analyzed each image in the software ImageJ using aboral spine density methods described below.

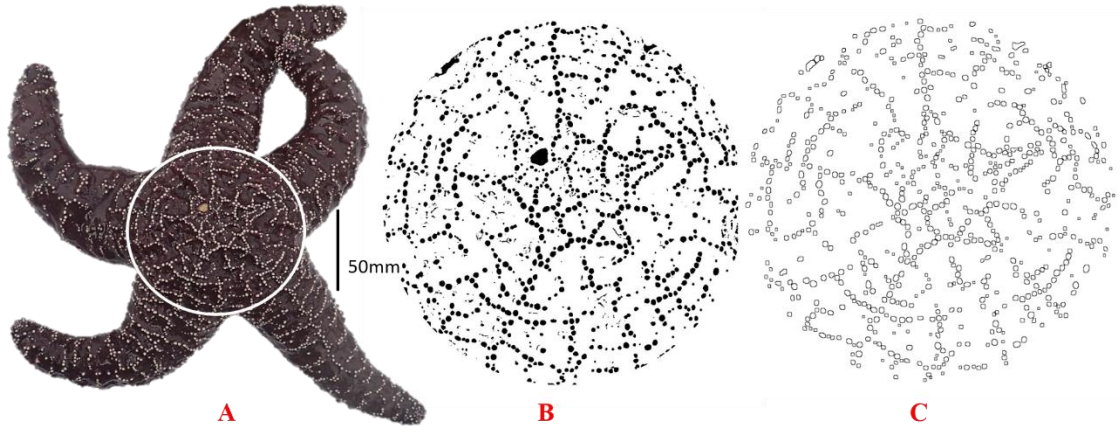

Figure 3. Planar view of digital images of *Pisaster ochraceus* used for aboral spine density estimation. (A) Central disc selection, (B) central disc isolation with reduction to 8-bit coloration for analysis, and (C) output image of noise reduction from macro batch protocols.

Aboral Spine Morphology

I modified previously established terminology from echinoid and asteroid spine anatomy to describe aboral spine morphology in *P. ochraceus* (Dubois and Ameye, 2001). Gross anatomical features of *P. ochraceus* spines include the head, shaft, and base (see Figure 4). I analyzed 400 individual spine samples from 75 sea stars from source locations: Control: PDZA (n =6); Boulder field sites PSG (n =11), FKC (n =10), and BB (n =10); Bay sites: DND (n =9), KS (n =10); and Bench sites: KH (n =10), and NH (n =9) to create four spine types. I also used a subset of the scanning electron micrographs (ten micrographs for each of the four spine types for a total of 40 spines of adult sea stars larger than 100 mm) to record spine anatomy measurements of (overall spine length, overall spine width, spine head length, and spine head width) in Software ImageJ. Lastly, I compared aspect ratios (spine length: width and spine head length: width) of the forty spines to the pre-defined spine types.

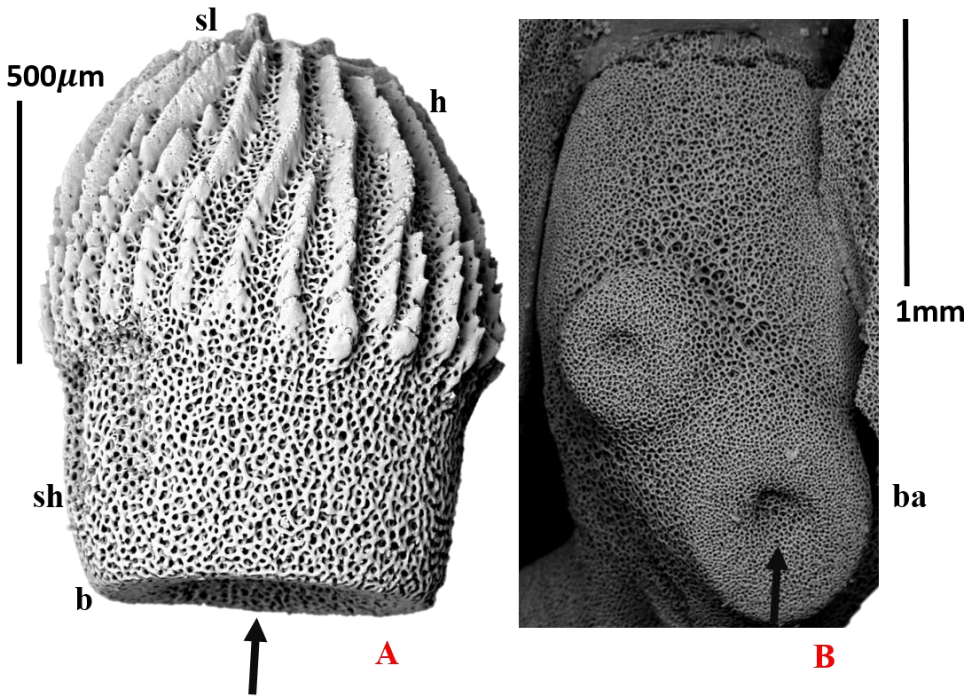

Figure 4. Scanning electron micrographs of a *Pisaster ochraceus* (A) aboral spine showing b: base with arrow pointing towards the invagination region for spine connection, sh: shaft, h: head, and sl: spinelets on the head; and (B) carinal ossicle showing ba: base attachment with arrow pointing towards the ligament and muscle attachment area.

After I removed each spine from the sea star, I placed it in an 8% sodium hypochlorite solution for 24 hours to remove all soft tissue. I rinsed the spines in distilled water and dried them in a drying oven at 75°C for 24 h. Dried spines were placed on a 12 mm scanning electron stub using a Pelcro™ carbon adhesive, which was then sputter coated using a Desk II Denton Vacuum Sputter Coater with a thin layer of gold. Scanning electron micrographs were taken to qualitatively analyze microscopic variation of the aboral spines. I captured all spine morphology with backscatter imaging at 20 to 25kV in the Quanta FEI 250 Scanning Electron Microscope at Humboldt State University. I used the software ImageJ to measure the length and width (mm) of the whole spine, spine head, spine shaft, and base width.

Associations Between Aboral Spine Density and Other *P. ochraceus* Traits

To examine associations between aboral spine variation and other sea star traits that function as protection from wave force, I measured sea star arm aspect ratio and attachment strength. I used arm aspect ratio, a trait previously quantified to be associated with wave exposure in *P. ochraceus*, to examine its relationship with aboral spine density (Hayne and Palmer, 2013). To do this, I used ImageJ (Schneider *et al.*, 2012) to measure the mean arm aspect ratio (Euclidean distance from the center of the central disc to the distal end of each ray divided by the width of each respective ray; Fig 5) of each sea star.

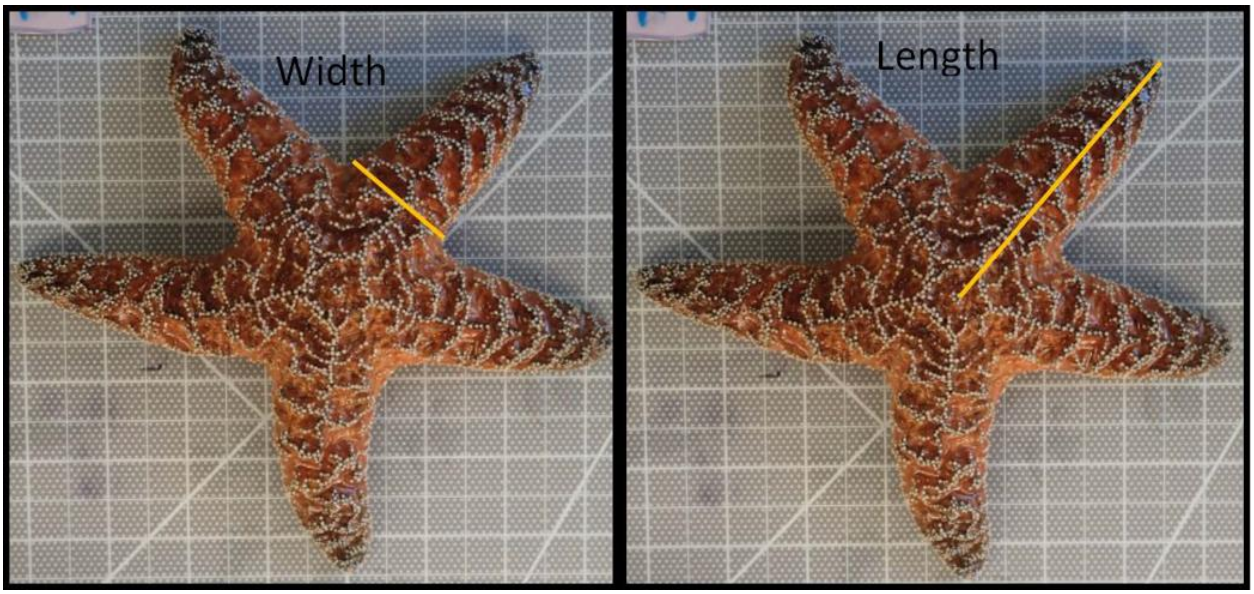

Figure 5. Digital images of *Pisaster ochraceus* showing arm aspect ratio (length: width) measurements.

To quantify sea star attachment strength via tube feet adhesion, I placed sea stars in a flow-through sea table. After a two-hour acclimation period, two perpendicular zip-ties were harnessed on each sea star in a crisscross pattern (Fig 6). Using a spring scale hooked under the harness, individual sea stars were removed at a 45-degree angle from the sea table surface and the force required to remove the sea star (i.e., displacement of the spring scale used to quantify attachment strength; Ferrer *et al.*, 2015) was recorded.

Figure 6. Attachment strength assay for *Pisaster ochraceus*. Two zip ties are fastened around the sea star (3D printed sea star replica shown in photograph) in a perpendicular fashion. A spring scale is hooked under both zip ties and the sea star is pulled at a 45º angle until it is removed from the surface.

Data Analysis

I used a simple Ordinary Least Squares (OLS) linear regression to examine the relationship between central disc aboral spines and whole sea star aboral spines to verify that aboral spine density on the central disc was an accurate proxy for aboral spine density on the whole sea star. I examined whether aboral spine density and spine size differed among habitats by using two separate Analysis of Covariance (ANVOCAs), with sea star radius as a covariate and habitat as a fixed factor. I also examined whether spine size differed among habitats by using ANCOVA with aboral spine density as a covariate and habitat as a fixed factor. I analyzed variation in the proportion of aboral spine shapes among habitats using MANOVA. Significant omnibus tests were followed by post-hoc pairwise comparisons (e.g., Tukey's HSD). When appropriate, data were log-transformed to meet assumptions of normality and linearity. Aboral spine microstructural variation was described qualitatively. All statistical analyses were done in R (R Core Team, 2013). I used a Multivariate Analysis of Variance (MANOVA) to test the hypotheses that spine measurements (overall spine length, overall spine width, spine head length, and spine head width) differed among habitat types. I followed the MANOVA with separate univariate tests on each spine measurement. I also used two separate ANCOVAs to examine the effects of sea star radius and habitat type on spine aspect ratio (spine length: width) and spine head aspect ratio (spine head length: width). To verify the spine categories that I developed, I tested whether spine aspect ratio and spine head ratio varied significantly among spine types using a one way ANOVA

RESULTS

Relationship Between Central Disc Aboral Spine Density and Whole Sea Star Aboral Spine Density

Using sea stars from four sites (PSG, FKC, DND, and KH), I found that the aboral spines on the central disc were significantly and positively associated with the spines on the entire aboral surface of each sea star (Figure 7, $y = 0.29x + 8.76$, $R^2 = 0.95$, $F_{1,12} = 268.4$, $P < 0.001$), indicating that the aboral spine density on the central disc was an accurate predictor of aboral spine density on the entire sea star.

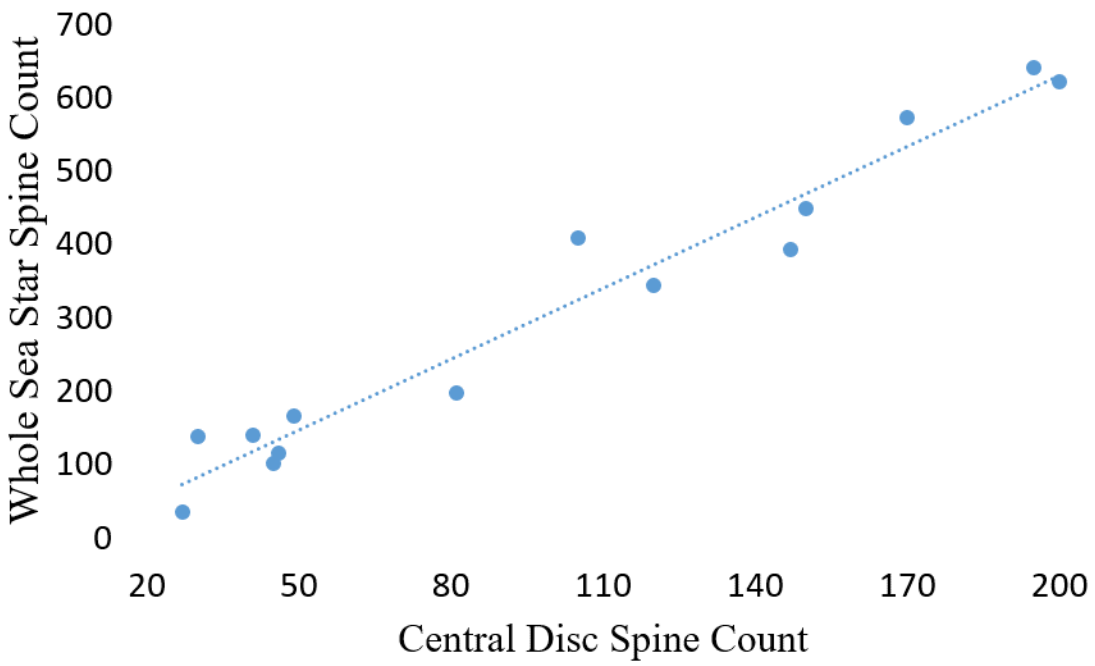

Figure 7. Relationship between spine number on the central disc and the spine number for the entire aboral surface of *Pisaster ochraceus*. Dotted line is OLS regression fit.

Aboral Spine Density and Mean Spine Area

In all habitats, aboral spine density decreased with increasing sea star radius, rapidly at first and then gradually decreased as sea stars got larger (Figure 8). ANCOVA of log-transformed data indicated that aboral spine density varied significantly with sea star size (star radius; (ANCOVA: $F_{1,159} = 41.46$, $P < 0.001$)), and across habitats ($F_{8,159} = 6.30$, $P = 0.002$), but the interaction between the two fell slightly out of significance, indicating that the relationship between spine density and sea star radius show similar slopes across habitats (ANCOVA: $F_{8,159} = 2.807$, $P = 0.063$). For the mean star radius, aboral spine density was highest at the boulder field habitat compared to the other habitats (Tukey's HSD, $P < 0.05$; Figure 9).

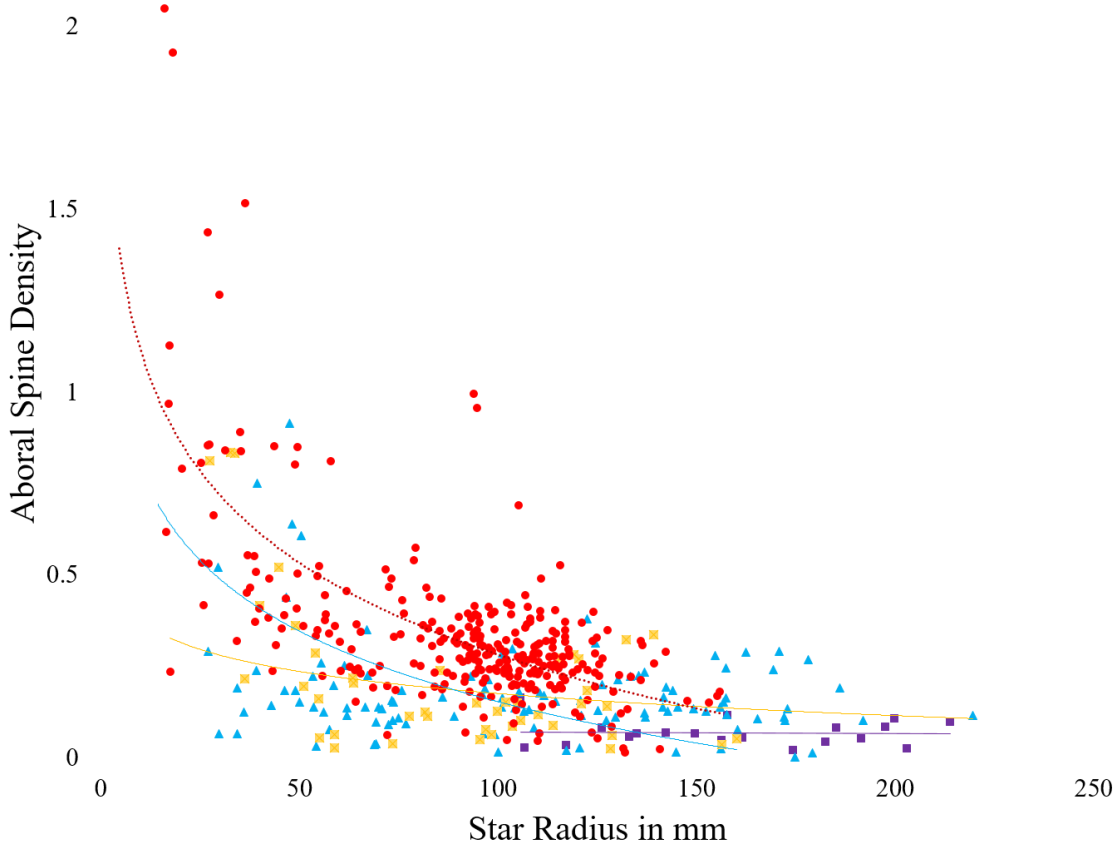

Figure 8. Relationship between radius (mm) and aboral spine density (no. spines · mm^{-2}) in *Pisaster ochraceus*. Color coding by habitat: Purple squares mark the benign control PDZA, yellow x's for bench habitat (SH, KH, and NH), red circles for boulder field habitat (PSG, FKC, PP, and BB), and blue triangels mark the bay habitat (KS and DND).

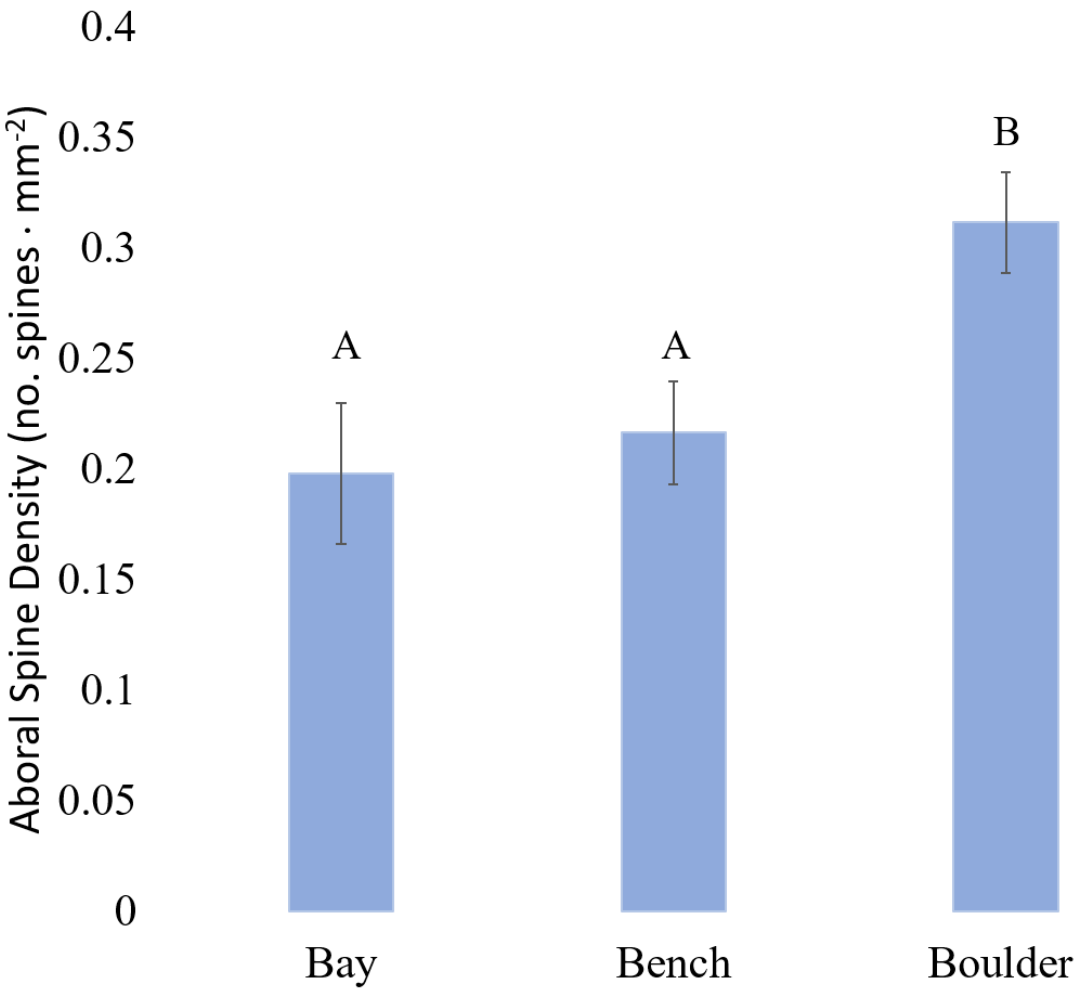

Figure 9. Mean (± SE) aboral spine densities of *Pisaster ochraceus* from each habitat at mean sea star radius (83.70mm). Different letters indicate significant differences between groups (Tukey HSD $P < 0.05$).

Among sea stars, there was a significant interactive effect of radius and habitat on spine size (ANCOVA: $F_{2,158} = 6.44$, $P = 0.002$), indicating that the relationship between spine size and sea star size was different among habitats. There was a significant effect of habitat on spine size (Figure 10; ANCOVA: $F_{2,158} = 13.70$, $P < 0.001$), but that effect depended on the radius of the sea star (ANCOVA: $F_{1,158} = 0.058$, $P = 0.81$). With respect to the relationship between spine size and spine density across habitats, spine size was significantly different across habitats (ANCOVA: $F_{1,158} = 16.08$, $P < 0.001$), and varied significantly as a function of spine density (ANCOVA: $F_{1,158} = 8.85$, $P = 0.003$), but the interaction was not significant (ANCOVA: $F_{2,158} = 0.66$, $P = 0.52$). For a given spine density, spines from sea stars at boulder fields were smaller compared to those from other habitats (Figure 11).

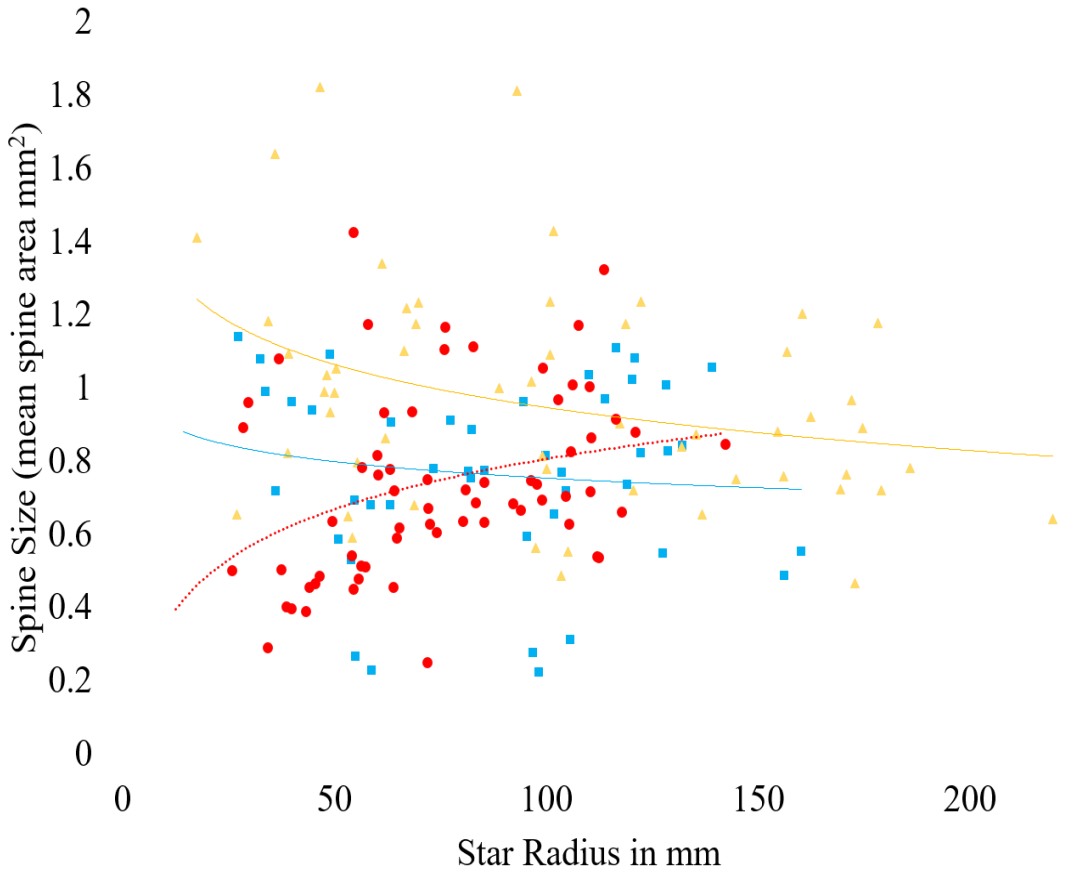

Figure 10. Relationship between radius (mm) and spine size (mean spine area in mm^2) in *Pisaster ochraceus*. Color coding by habitat location: yellow triangles represent the bench habitat (SH, KH, and NH), red circles for the boulder field habitat (PSG, FKC, PP, and BB), and blue squares mark the bay habitat (KS and DND).

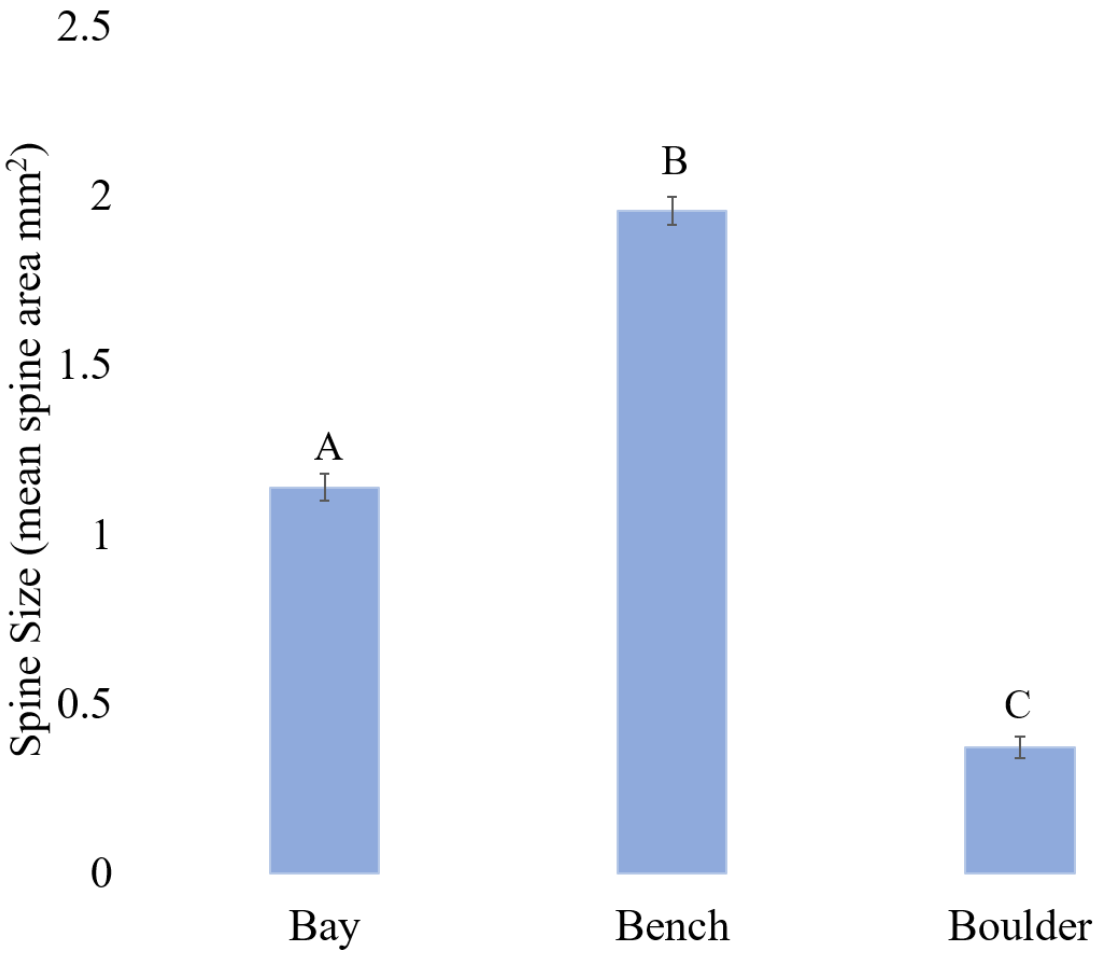

Figure 11. Mean central disc spine size ([Sum of central disc spine area · central disc area^{-1}) · 100]) (± SE) of *Pisaster ochraceus* from each habitat at mean aboral spine density (0.26). Different letters indicate significant differences between groups (Tukey HSD $P < 0.05$).

Aboral Spine Morphology

I found that the head of each aboral spine contained spinelets, which are thickened calcium carbonate structures that protrude from the head in an upright orientation and are located in the center of the head and descend towards the shaft (see Figure 3A). I use the 'head' classification because it was the only region not previously described or categorized but an integral part of *P. ochraceus'* aboral spine anatomy. The shaft was characterized as the middle columnar portion of the spine, which lacks spinelets (see Figure 3A). The base of the spine formed the bottom of the spine column with a small central invagination (see Figure 3A), which was an insertion point for ligament-like connective tissues banding musculature that connects to the carinal ossicle (see Figure 3B). Asteroid spine bases were different from an echinoid-like spine anatomy, in that they lacked the milled ring for muscle attachment and connected to the carinal ossicle as a mirrored cylinder as opposed to a ball and socket-like connection. Spines in *P. ochraceus* were different from spines previously published in asteroids as they were found to be wide, possessed thick spinelet ridges, and an obvious (and aforementioned) head region (Dubois and Ameye 2001; Mooi 1986).

I found four aboral spine shapes in *P. ochraceus* among my collection sites: columnar, spade, blunt, and convex. Columnar spines were erect or upright spines that contain a head region that is of similar width to the shaft (Fig 12A). The columnar spines had the highest spine ratio of any of the spines, which showed that columnar spines were significantly taller and narrow (Fig 13 left panel). The head region also had a high head

spine ratio, but was not significantly different from the ‘spade’ spine type which is also an upright form (Fig 13 right panel). Spinelets on the spine head of columnar spines are repeating wedges that form thin rows that were oriented in either a symmetrical or a sporadic fashion (Fig 14A and B). Columnar spines were by far the most common aboral spine type in sea stars at PDZA, but were only found in small numbers on sea stars at BB, DND, KS, and NH (Fig 15). Juvenile columnar spines, found at KS, are upright with tall, uniform wedges. Each wedge is separate and does not form ridges (Fig 14C).

Spade spines (Fig 12B) are upright spines with a particular head shape: the top of the head is narrow to a point and widens to the connected region of the shaft. The spine ratio is significantly different from all the other spine types (Fig 13 left panel). The portion of the head closest to the shaft is the widest point of the spine, but the ratio is still taller than wide (Fig 13 right panel). Spinelets consisted of simple rows with some dentate ridges that form minor peaks (Fig 14 C, D, and F). The spade spine type was found in sea stars at all collection sites (Fig 12).

Blunt spines were the least common spine type across all collection sites (Fig 12), and were not a dominant spine type for any individual sea star. Blunt spines (Fig 12 C), consist of a squat or flattened head region that is almost equal in width to the spine shaft (Fig 13). Blunt spinelets are highly variable from thin and dentate, to thick with smooth ridges (Fig 14 A-D and F). Juveniles were observed with this spine type at BB and PSG with thick, smooth ridges (Fig 15 A).

Convex spines were found at significantly higher at bench and boulder field locations. Convex spines are named for the mushroom-shaped head which looks like a

distinct cap-like structure that extends laterally (Fig. 12). The convex spine type was not significantly different in spine or spine head ratio (Fig 13). Convex spines were the dominant type in 46 individuals, which accounted for more than half of all samples. The variation of the spinelets in convex spines were higher than other spine types, with ridges that were either simple, dentate, or completely porous (Fig 14 C-F), resulting in numerous, narrow columns in ridge-like organization (Fig 14 G-H). Juveniles with convex spine types had large ridges that fanned out from the head more than any other spine type (Fig 15 B).

The relative proportions of spine types were significantly different across habitat types (MANOVA, $F_{3,71} = 8.98$, $P < 0.001$; Fig 16). Sea stars with a larger proportion of the 'convex' spine type were more prevalent in bench and boulder field habitats than in bay habitats (post-hoc univariate ANOVAs, $P < 0.001$ for both bench and boulder field, Fig 16). Bay sea stars had a significantly larger proportion of 'spade' spines than in bench and boulder field habitats (Fig 17).

In respect to spine anatomy, spine ratios (spine length to spine width) was significant across habitats (ANCOVA, $F_{2,61} = 7.79$, $P < 0.001$) and sea star radius ($F_{1,61} = 18.597$, $P < 0.001$), but non-significant habitat effects for the univariate tests on each spine measurement. Lack of significant habitat effects in the univariate tests suggests that the current amount of data is insufficient to reach any confident conclusion regarding any of the individual spine measurements. I found that bay sea stars had a significantly higher spine ratio: bay sea star spines were taller than wide (Fig 17, Tukey $P < 0.001$). Boulder field and bench sea stars had spines that were closer to a 1:1 ratio and significantly

different from bay sea stars (post hoc Tukey $P < 0.001$). Bench sea star spines were not significantly different from bay or boulder field habitat, with respect to spine head ratios (Figure 17 left panel).

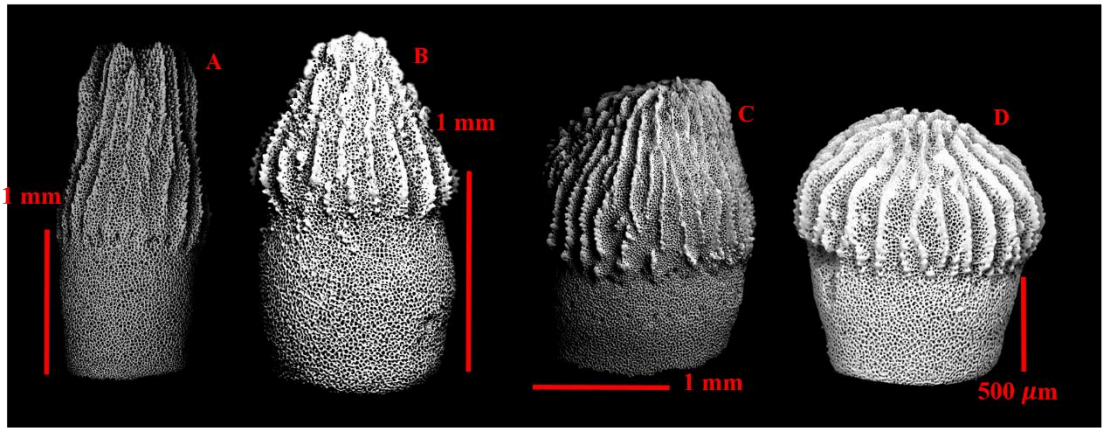

Figure 12. Scanning electron micrographs of adult aboral spine types in *Pisaster ochraceus*. (A) Columnar, (B) spade, (C) blunt, and (D) convex.

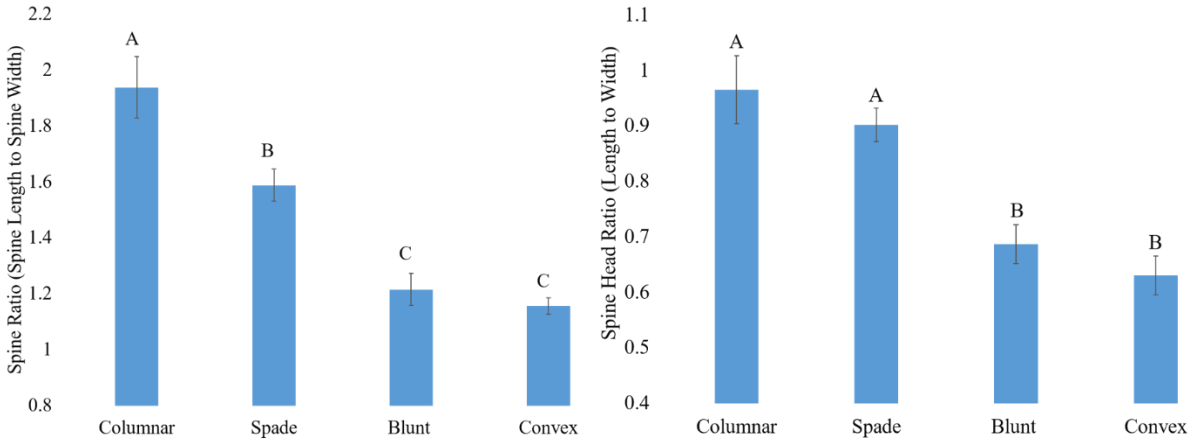

Figure 13. Mean (± SE) whole spine ratio (spine length: spine width) (left) and spine head ratio (head length: head width) (right) for each spine type in adult *Pisaster ochraceus*. Different letters indicate significant differences between groups (Tukey HSD $P < 0.05$).

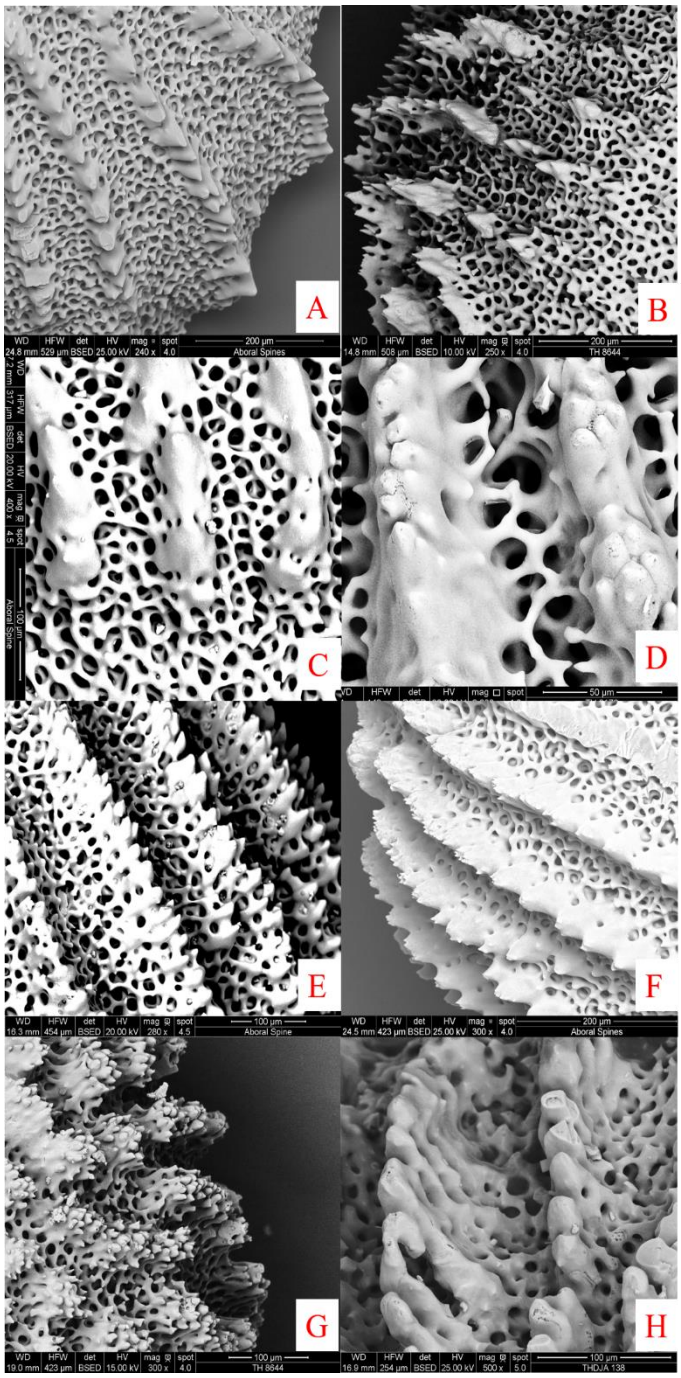

Figure 14. Scanning electron micrographs of distinct spinelet types in *Pisaster ochraceus*: (A) thin wedges, (B) sporadic ridges, (C) smooth ridges, (D) globular ridges, (E-F) dentate ridges, and (G-H) porous, complex ridges.

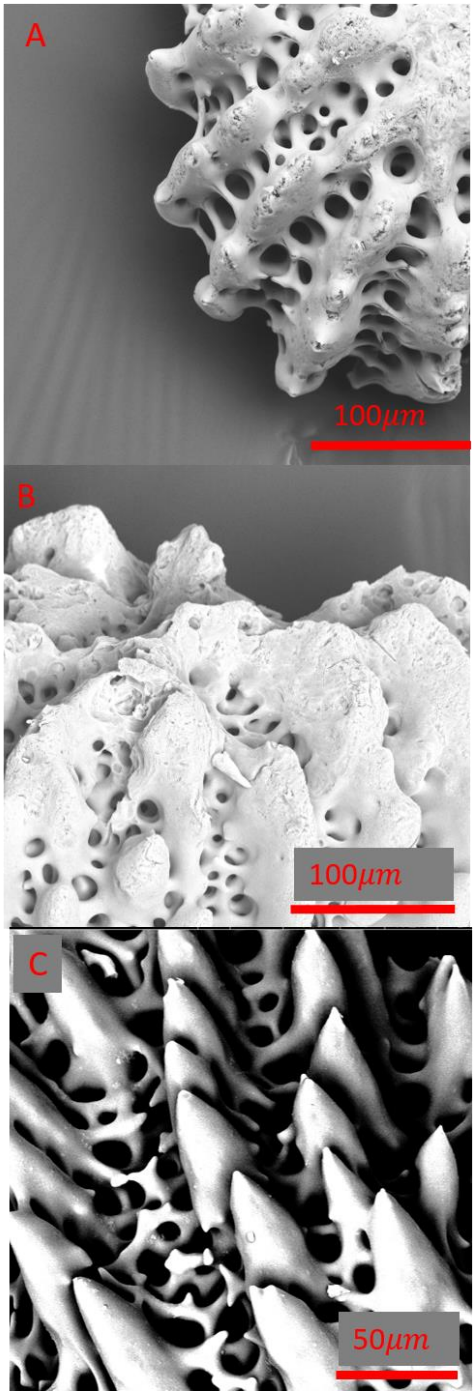

Figure 15. Scanning electron micrographs showing juvenile spinelet variation in *Pisaster ochraceus*. (A) thick with smooth ridges, (B) large, with thick fan-like ridges, and (C) separate wedges with pointed barbs on each tip.

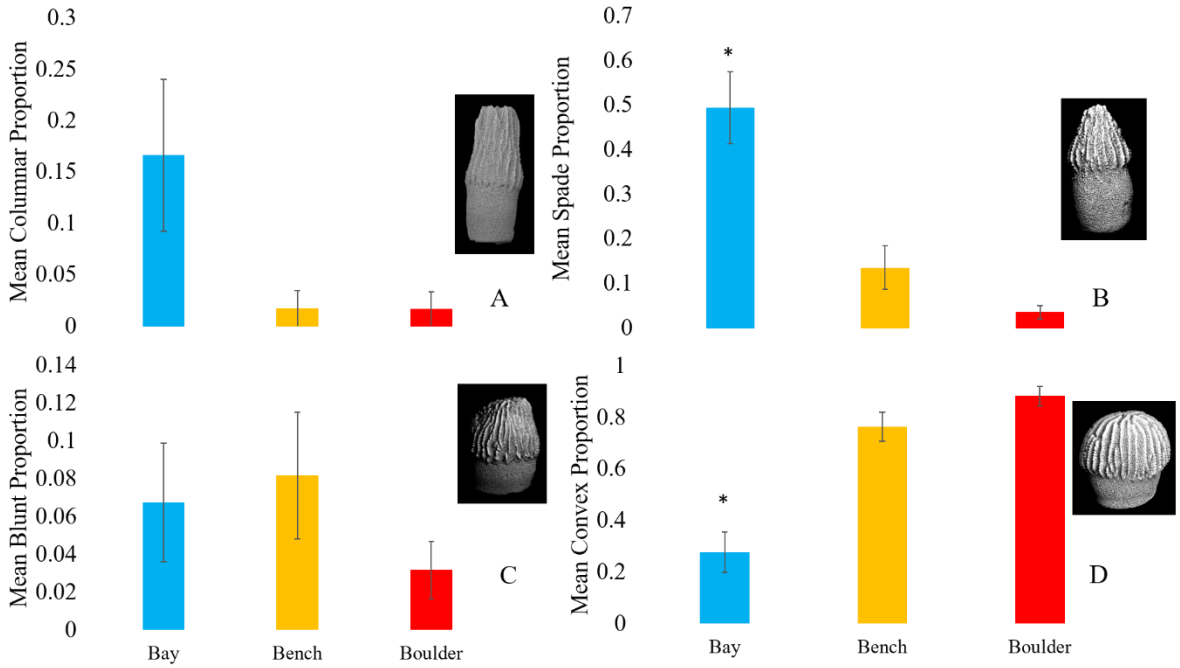

Figure 16. Mean (± SE) proportion of each of the spine type for *Pisaster ochraceus* from bay, bench, and boulder habitats. Panel A represents columnar spines with a columnar spine for representation; panel B represents spade spines, C for blunt spines, and D for convex spines. Asterisks represent statistical differences in spade and convex spines between sea stars from bay habitats and both bench and boulder field habitats.

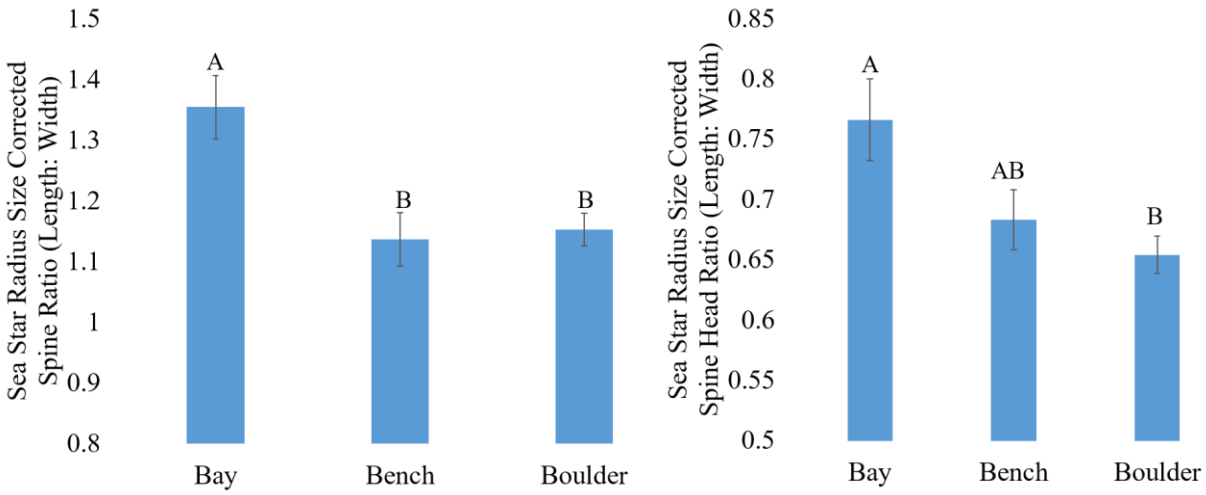

Figure 17. Left: Mean (± SE) radius-adjusted whole spine ratio (spine length: width) (left) and spine head ratio (head length: head width) in *Pisaster ochraceus* across habitat types. Different letters indicate significant differences between groups (Tukey HSD $P < 0.05$).

Associations Between Aboral Spine Density and Other P. ochraceus Traits

I found no significant relationship between aboral spine density and attachment strength in *P. ochraceus* (Fig 18; OLS Linear Regression $F_{1,20} = 1.36$, $P = 0.257$). Aboral spine density was also not significantly associated with arm aspect ratio (OLS Linear Regression $F_{1,37} = 2.94$, $P = 0.095$, Fig 19).

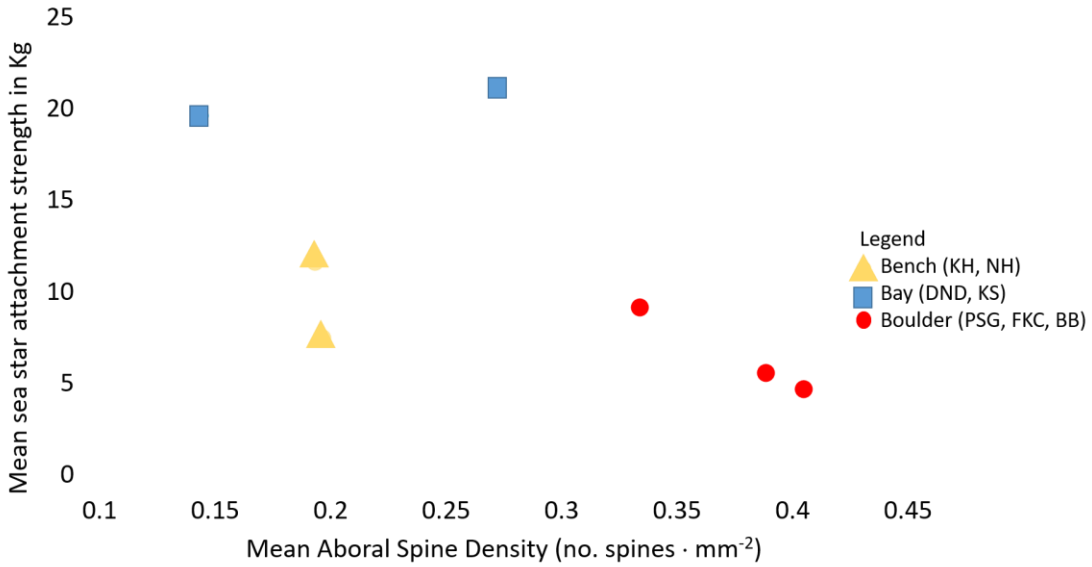

Figure 18. Relationship between mean aboral spine density and mean sea star attachment strength (in kg) per site in *Pisaster ochraceus*. Data points color-coded by habitat type: blue squares represent bay habitat, yellow triangles mark the bench habitat, and red circles mark the boulder field habitat. (Ordinary least squares linear regression $R^2 = 0.25$, $F_{1,20} = 1.36$, $P = 0.257$).

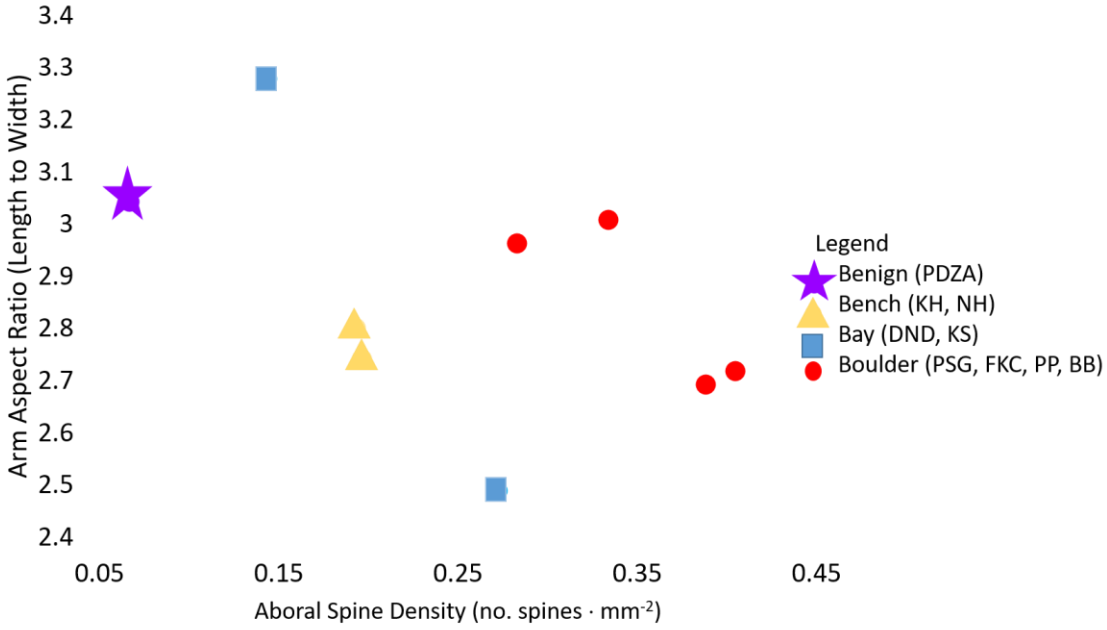

Figure 19. Relationship between mean spine density and mean arm aspect ratio (arm length: width) per site in *Pisaster ochraceus*. Data points color-coded by habitat type: PDZA reference sites represented as a purple star, blue squares represent bay sites, yellow triangles mark the bench habitat, and red circles mark the boulder field habitat type. (Ordinary least squares linear regression R^2 =0.04, $F_{1,6}$ = 1.27, P =0.302).

DISCUSSION

Individual *P. ochraceus* varied significantly with respect to aboral spine density, spine size, and morphology. First, aboral spines in *P. ochraceus* appear to exhibit ontogenetic variation. Specifically, aboral spine density was higher in smaller sea stars than in larger sea stars at all sites. Thus, spines may play a more important protective role in juvenile stars compared to adults, as smaller sized stars may be more vulnerable to wave-carried projectiles, sediments, or predators. Alternatively, it is possible that aboral spine growth occurs at a faster rate in juvenile *P. ochraceus*, as smaller individuals in this species grow faster than larger individuals (Gooding, *et al.* 2009).

The habitat-specific aboral spine variation that I observed has the potential to result from adaptive variation in response to wave-related stress. Habitat-specific variation in traits associated with protection from wave-exposure is consistent with the findings of previous studies on *P. ochraceus*, where individuals from wave-exposed habitats had thinner, flatter bodies and higher attachment strength than their wave-protected counterparts (Hayne, 2011; Hayne and Palmer, 2013). Interestingly, these wave-exposed individuals were also noted to be ‘spinier’ (Hayne and Palmer, 2013); however, my analysis of the relationships between aboral spine density and arm aspect ratio and attachment strength found no significant associations among these traits. For example, sea stars in the protected bay habitat were unexpectedly stronger than seas stars from other habitats (Appendix A). The lack of association between spine density and arm aspect ratio and attachment strength suggest that a spinier morphology may not be

adaptive for wave-exposure *per se*. Instead, I hypothesize that a denser covering of aboral spines functions as protection from dermal abrasion in environments that are wave-exposed but also have large amounts of coarse sediment.

With respect to aboral spine shape, I quantified four spine types: columnar, spade, blunt, and convex. However, research is needed to understand the variability that I have quantified. I do not know if the spine types represents a gradient or distinct spine types. Given that, I found sea stars from sites where convex spines were the dominant spine type also had higher spine density. The convex spine type is the most extreme spine shape of any of the spines that I categorized; short spines with a wide head shape that extends laterally forming a cap-like structure. This spine type is atypical among most echinoderm spines, but is at least superficially similar to the flattened head shape of aboral spines of the shingle urchin *Colobocentrotus atratus* (Chen, 2011). In the shingle urchin, the flattened aboral spine shape aids in survival in extreme intertidal wave-exposed environment by reducing drag forces. The convex structure of the spine could also aid in protection from predators (as in the flat, armored spines of valvatacean sea stars; Blake 1983).

Both spine density and morphology were significantly different among habitats. Sea stars in protected environments had spines that were more upright and lacked protrusions, while in the exposed habitats (boulder and bench); the convex spine was the dominant spine type. As bench and boulder field locations are subject to both abrasion from suspended particulates and wave shock, the convex aboral spine shape, in conjunction with a dense covering, may provide a ‘canopy-like’ function that protects the

sea star from dermal abrasion. Spine canopies can be found in the Order Clypeasteroidae (sand dollars and allies), which have miliary spines (Mooi, 1986). In the genus *Eucidaris*, the tip of the miliary spine is filled with additional epithelial tissue, creating a club shape. These densely-packed spines create a 'spine canopy' (beneath the top layer of primary spines) that blocks larger suspended particles from contacting the test and generates a ciliary current to keep fine particles away from the dermal surface and keeps the epithelium clean and well ventilated, thus facilitating respiration in turbid water (Mooi, 1986). The convex spines in *P. ochraceus* could function similarly to the miliary spines of clypaesterids that protect the aboral surface from large and small particles. Sea stars that reside in boulder field habitats may benefit from a dense covering of convex spines more so than sea stars in other habitat types, because the small boulder and cobble habitat in which they reside incr.00eases proximity to suspended particles and sediment. Further, data collected from some of my field sites suggests that boulder field habitats have more suspended sediment in the water column than at bench and bay sites (Appendix B).

It is currently not known whether the aboral spine variation I observed is due to ecophenotypic plasticity or to heritable polymorphism. *P. ochraceus* has been previously shown to exhibit at least two phenotypically plastic traits that vary with exposure to wave action: thinner body form and increased tube foot strength in exposed waters (Hayne and Palmer, 2013; Hayne, 2011). Because of this, it is possible that aboral spine density and morphology are additional phenotypically plastic traits that are modified in accordance with the local wave environment. Documenting associations between aboral spine variation and wave action and a subsequent common-garden experiment transplanting sea

stars among wave-exposed and wave-protected habitats would be necessary to determine whether aboral spine variation is a result of environmental or genetic control.

There are several alternative possibilities for the habitat-specific aboral spine variation I observed. One possibility is antipredator protection. High aboral spine density could function as mechanical protection, influence palatability, or act as camouflage. Predators of *P. ochraceus* are somewhat scarce, with observations limited mainly to gulls to sea otters (Grizmek, 1972). In the duration of my study from 2015 to 2018, observations of predation upon *P. ochraceus* was extremely rare across all habitat types. Further, neither gulls nor otters are common in the habitats I surveyed. Because of this, I do not believe that the aboral spine variation in local *P. ochraceus* function to combat predation. Another possibility is that variable aboral spine density in *P. ochraceus* is an energetic by-product produced by a trade off against soft-tissue growth. For example, Feder (1970) noted that *P. ochraceus* in calm environments that were able to consume more food, had in thicker arms, more visible soft tissue, and fewer aboral spines. It may be that sea stars in protected embayments and on rocky benches where sessile prey (e.g., barnacles and mussels, Appendix C) are more abundant, are allocating more energy to soft tissue than skeletal elements like aboral spines (Gooding and Harley, 2009). Sea stars in boulder fields may have to spend more time searching for scarcer, mobile, and less profitable prey (e.g., snails, limpets, and chitons) and therefore have a 'skin and bones' look with less soft tissue and more visible skeletal elements. Because of the variable nature of food availability and quality across habitat types in my study, it is possible that sea star condition is influencing aboral spine variation. However, using volumetric

reconstructions of a ‘spinier’ and ‘nonspiny’ sea star shows that the ‘spinier’ appearance does equate to less soft tissue, but an increase of aboral spines (Appendix D). Future studies should address the precise mechanism underlying aboral spine growth.

A potential benefit of understanding variation in aboral spine density in sea stars, is that the combination of aboral spine density and orientation appear to form a unique pattern on the aboral surface of individual sea stars. For example, in juveniles, spines form a five-pointed ‘star’ shape in the center of the central disc, in line with the madeporite, with a thin row of spines that radiate away from the central disc ‘star’ down each ray. Larger individals have banded spine patterns in their rays that are perpendicular to the center of the central disc ‘star’ and extend toward the ray tip. Interestingly, I observed that spines on adult sea stars with low spine densities tend to retain this juvenile spine pattern, or possess a slight modification of this pattern with a loss of the ray midline in favor or small clusters on the top margins of the arm similar to the banding I describe above (Fig 1). It appears that most of the original spine pattern, at least the central disc portion of the sea star, in the juvenile remains throughout adulthood, but future research is necessary to quantify this. Sea stars with higher spine densities also possess numerous centric patterns of spines that fall in the inter-radial regions on the central disc. Such individual differences or ‘fingerprints’ could be used as a way to non-invasively indentify individual sea stars in a similar fashion to how other organisms with varying densities and patterns of surface structures are identified (e.g., whale sharks, Arzoumanian *et al.*, 2005). During my study, I successfully used the unique aboral spine patterning to identify individual sea stars as a back up to ensure that individuals were not misidentified through

observer error. This technique could be useful in projects that track individuals over time, and has not been previously explored as a potential identification protocol for *P. ochraceus* (Hayne, 2011).

My methods for quanitifying aboral spine variation are easily repeatable, with the potential to be used to investigate intra- and inter-specific aboral spine variation in other asteroid species. The high degree of intraspecific variation that I found across collection sites suggests the potential for habitat-specific spine phenotypes, and adaptive variation in aboral spines of *P. ochraceus*. However, more research is needed to examine such possibilities.

REFERENCES

Arzoumanian, Z., Holmberg, J., & Norman, B. (2005). An astronomical pattern-matching algorithm for computer-aided identification of whale sharks *Rhincodon typus*. *Journal of Applied Ecology*, *42*(6), 999-1011.

Bell, E. C., & Denny, M. W. (1994). Quantifying "wave exposure": a simple device for recording maximum velocity and results of its use at several field sites. *Journal of Experimental Marine Biology and Ecology*, *181*(1), 9-29.

Chen, T. T. (2011). Microstructure and micromechanics of the sea urchin, *Colobocentrotus atratus* (Doctoral dissertation, Massachusetts Institute of Technology).

Clark A.M. (1996) An index of names of recent Asteroidea. Part 3: Velatida and Spinulosida. In Jangoux M. and Lawrence J. (eds)

Cohen-Rengifo, M., Agüera, A., Detrain, C., Bouma, T. J., Dubois, P., & Flammang, P. (2018). Biomechanics and behaviour in the sea urchin Paracentrotus lividus (Lamarck, 1816) when facing gradually increasing water flows. *Journal of Experimental Marine Biology and Ecology*, *506*, 61-71.

Denny, M., & Gaylord, B. (1996). Why the urchin lost its spines: hydrodynamic forces and survivorship in three echinoids. *Journal of Experimental Biology*, *199*(3), 717-729.

Denny, M. (2014). *Biology and the mechanics of the wave-swept environment* (Vol. 917). Princeton University Press.

Doty, M. S. (1971). Measurement of water movement in reference to benthic algal growth. *Botanica Marina*, *14*(1), 32-35.

Dubois, P., & Ameye, L. (2001). Regeneration of spines and pedicellariae in echinoderms: a review. *Microscopy Research and Technique*, *55*(6), 427-437.

Eylers, J. P. (1976). Aspects of skeletal mechanics of the starfish *Asterias forbesii*. *Journal of Morphology*, *149*(3), 353-367.

Feder, H. M. (1970). Growth and predation by the ochre sea star, *Pisaster ochraceus* (Brandt), in Monterey Bay, California. *Ophelia*, *8*(1), 161-185.

Fisher, W. K. (1930). Asteroidea of the North Pacific and adjacent waters pt. 3: Forcipulata (concluded). *Bulletin of the United States National Museum,* 148-436.

Frontana-Uribe, S., De la Rosa-Velez, J., Enríquez-Paredes, L., Ladah, L. B., & Sanvicente-Anorve, L. (2008). Lack of genetic evidence for the subspeciation of *Pisaster ochraceus* (Echinodermata: Asteroidea) in the north-eastern Pacific Ocean. *Journal of the Marine Biological Association of the United Kingdom*, *88*(2), 395-400.

Gooding, R. A., Harley, C. D., & Tang, E. (2009). Elevated water temperature and carbon dioxide concentration increase the growth of a keystone echinoderm. *Proceedings of the National Academy of Sciences*, *106*(23), 9316-9321.

Hayne, K. (2011). Plastic phenotypic responses of the sea star *Pisaster ochraceus* to spatial and temporal variation in wave exposure. (Doctoral dissertation, University of Alberta).

Hayne, K. J., & Palmer, A. R. (2013). Intertidal sea stars (*Pisaster ochraceus*) alter body shape in response to wave action. *Journal of Experimental Biology*, *216*(9), 1717-1725.

Jokiel, P. L., & Morrissey, J. I. (1993). Water motion on coral reefs: evaluation of the'clod card'technique. *Marine Ecology Progress Series, 93,* 175-181.

LeClair, E. E. (1993). Effects of anatomy and environment on the relative preservability of asteroids: a biomechanical comparison. *Palaios*, 233-243.

Menge, B. A. (1976). Organization of the New England rocky intertidal community: role of predation, competition, and environmental heterogeneity. *Ecological Monographs*, *46*(4), 355-393.

Menge, B. A. (1992). Community regulation: under what conditions are bottom-up factors important on rocky shores? *Ecology*, *73*(3), 755-765.

Mooi, R. (1986). Structure and function of clypeasteroid miliary spines (Echinodermata, Echinoides). *Zoomorphology*, *106*(4), 212-223.

Paine, R. T. (1969). The *Pisaster-Tegula* interaction: prey patches, predator food preference, and intertidal community structure. *Ecology*, *50*(6), 950-961.

Palumbi, S. R. (1984). Tactics of acclimation: morphological changes of sponges in an unpredictable environment. *Science*, *225*(4669), 1478-1480.

Raimondi, P. T., Sagarin, R. D., Ambrose, R. F., Bell, C., George, M., Lee, S. F & Murray, S. N. (2007). Consistent Frequency of Color Morphs in the Sea Star Pisaster ochraceus (Echinodermata: Asteriidae) across Open-Coast Habitats in the Northeastern Pacific1. *Pacific Science*, *61*(2), 201-211.

Ricketts, E. F., Calvin, J., Hedgpeth, J. W., & Phillips, D. W. (1985). *Between pacific tides*. Stanford University Press.

Sanford, E., & Kelly, M. W. (2011). Local adaptation in marine invertebrates. *Annual review of marine science*, *3*, 509-535.

Schiel, D. R., Wood, S. A., Dunmore, R. A., & Taylor, D. I. (2006). Sediment on rocky intertidal reefs: effects on early post-settlement stages of habitat-forming seaweeds. *Journal of Experimental Marine Biology and Ecology*, *331*(2), 158-172.

Thompson, T. L., & Glenn, E. P. (1994). Plaster standards to measure water motion. *Limnology and Oceanography*, *39*(7), 1768-1779.

Toubarro, D., Gouveia, A., Ribeiro, R. M., Simões, N., Da Costa, G., Cordeiro, C., & Santos, R. (2016). Cloning, characterization, and expression levels of the nectin gene from the tube feet of the sea urchin *Paracentrotus Lividus*. *Marine Biotechnology*, *18*(3), 372-383.

Tsafnat, N., Gerald, J., Le, H. N., & Stachurski, Z. H. (2012). Micromechanics of sea urchin spines. *PLoS One*, *7*(9), e44140.

Wentworth, C. K. (1922). A scale of grade and class terms for clastic sediments. *The Journal of Geology*, *30*(5), 377-392.

APPENDICES

APPENDIX A

Sea Star Strength Assay

Mean sea star attachment strength by habitat shows significantly higher strengths in sea star *P. ochraceus* at bays sites compared to bench and boulder sites (Fig 20). Size (sea star radius; (ANCOVA $F_{1,79} = 13.565$, $P < 0.001$) and habitat ($F_{2,79} = 19.307$, $P < 0.001$) are significant factors in analyzing sea star attachment strength, but the interaction was not significant ($F_{2,75} = 1.753$, $P = 0.18$). Tukey-Kramer test shows Bay sea stars are significantly stronger than the other two habitats. Using the mean sea star radius, sea stars in the bay habitat were as much as four times stronger than the other habitats (Fig 21).

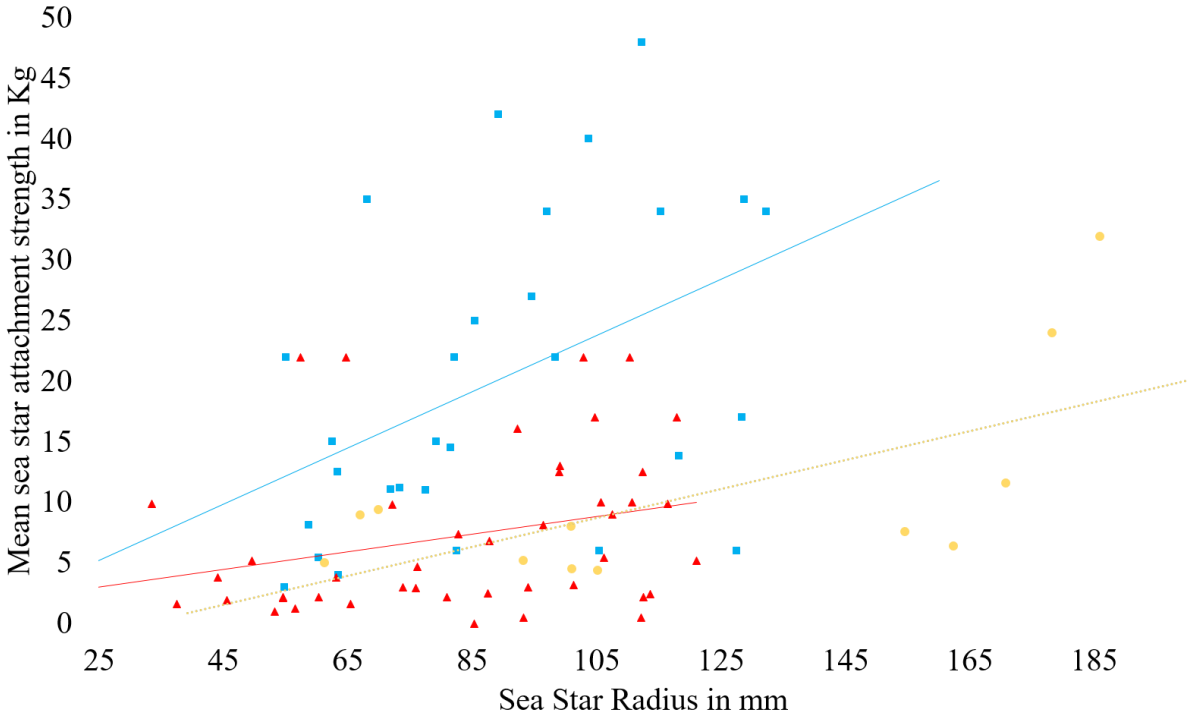

Figure 20. Relationship between sea star attachment strength (in kg) and sea star radius (in mm) as sea star removal from substrate (flat tank surface).

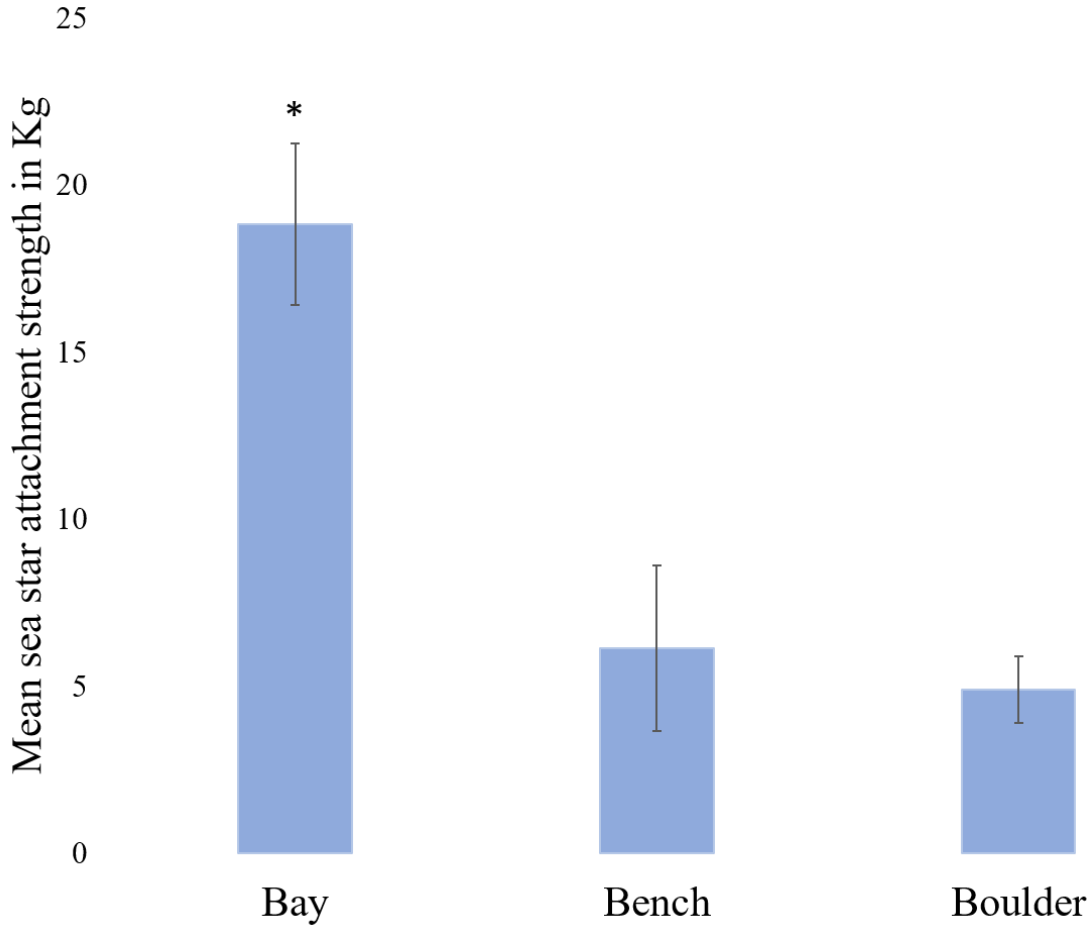

Figure 21. Sea star attachment strength in Kg for the mean sea star radius across sites. Bay is significantly stronger as represented by the asterisk.

APPENDIX B

Environmental Variation of Abiotic and Biotic Factors among Representative Habitats

To assess abiotic environmental variation associated with each habitat type, I installed an array of devices to measure water motion and abrasion stress at a representative boulder site (PSG), two bench sites (KH and NH), and one bay site (KS) in July 2018. Arrays consisted of a sediment trap and a clod card (Thompson and Glenn, 1994). I deployed two to three arrays in the mid to low zones where *P. ochraceus* were abundant (Figure 22). Sediment traps were made of J-shaped PVC pipes of 4 cm internal diameter and 45cm length with a height-to-mouth diameter (H/D = 11.25), which is an optimal proportion for sediment sampling in rocky intertidal zones as it is between 10 to 15 (Shiel *et al.*, 2006). I collected sediment daily from each of the traps. Using size 4 Φ sieve plates, I filtered the total site sediment to separate large sand particles from clay and silt, to isolate the larger particles that can cause abrasion to *P. ochraceus* (Wentworth 1922). I quantified grams of sand per trap per day for a daily sedimentation rate for each site. Clod cards, which have been used previously to measure water motion (Doty, 1971; Jokiel and Morrissey, 1993), were made of plaster of Paris (size 3.5cm^3). I measured each dry clod card before and after deployment, and monitored them in the field to ensure collection before complete dissolution. I quantified water motion as clod card loss in g averaged per day for each site.

Figure 22. Digital images of abiotic stressor arrays installed in the rocky intertidal zone. Each abiotic array contained one plaster of Paris block (i.e., clod card), and one J-shaped sediment trap.

In general, the rock bench collection sites (NH and KH) had the highest clod card dissolution per day with 61.6g and 43.3g, respectively; indicating that water motion was greatest at the bench sites compared to the bay and boulder sites. However, only NH was significantly different from the bay site KS and boulder site PSG (Fig 23; One way ANOVA $F_{3,18} = 8.174$, $P = 0.0027$; KS; Tukey: $P = 0.002$; PSG, $P = 0.006$). KS had the least amount of clod card dissolution, with an average of 23.8g lost per day. The boulder field site (PSG) had clod card loss of 30.9g.

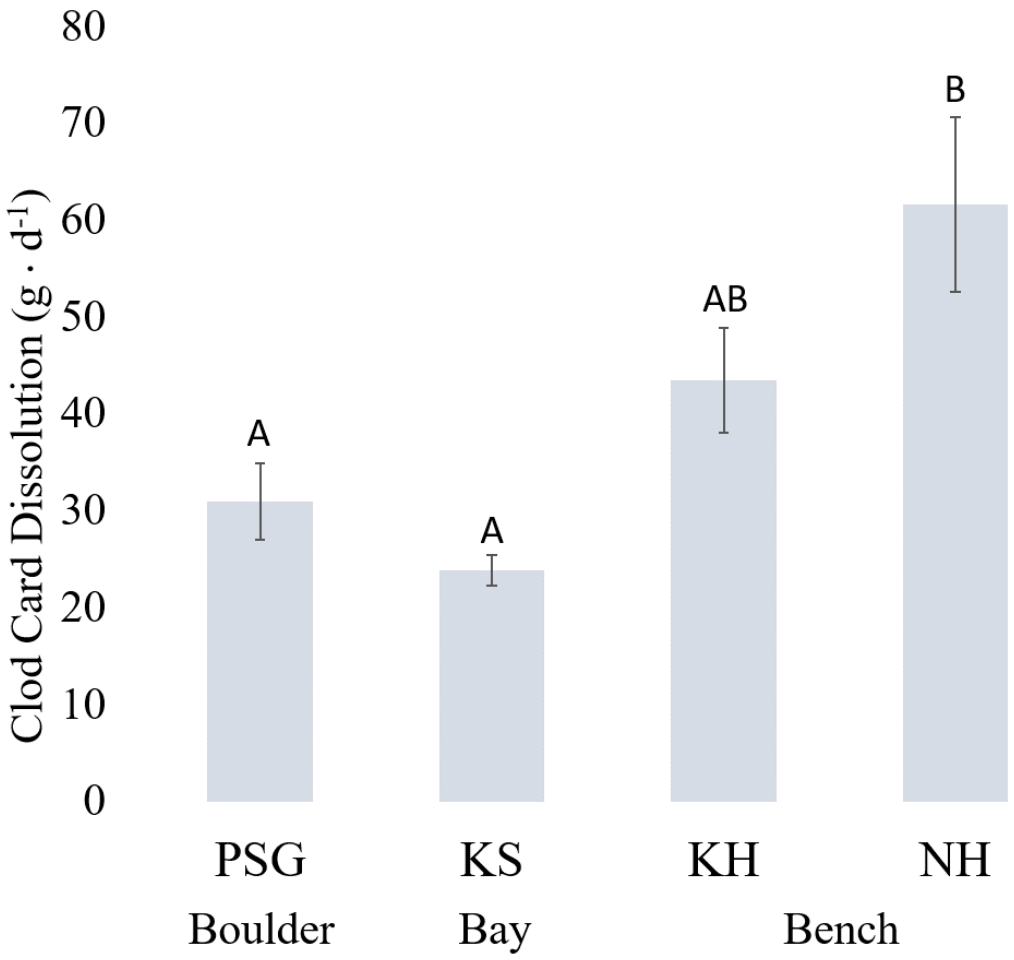

Figure 23. Mean (± SE) clod card dissolution ($g \cdot d^{-1}$) at each representative habitat site (One way ANOVA $F_{3,18} = 8.174$, $P = 0.0027$). Dissolution at NH was significantly higher than PSG (Tukey: $P = 0.002$) and KS (Tukey: $P = 0.002$). Site initials as follows: Point St George (PSG), King Salmon (KS), Kibesillah Hill (KH), and Noyo Headlands (NH).

The boulder field site (PSG) had the highest sediment accumulation of any site, with an average of 39.75g per trap per day (Fig 24; One way ANOVA $F_{3,6} = 121.6$, $P = 9.22 \times 10^{-6}$). Using a Tukey's multiple comparisons of means, PSG was different from KS ($P = 4.04 \times 10^{-5}$), KH ($P = 2.57 \times 10^{-5}$), and NH ($P = 1.28 \times 10^{-5}$). Only trace amounts of sediment were collected in the traps at the bay site (KS), with 0.58g per trap per day. During the duration of the sediment trap deployment, I did not find any sediment accumulated in any of the traps at either bench site (NH and KH).

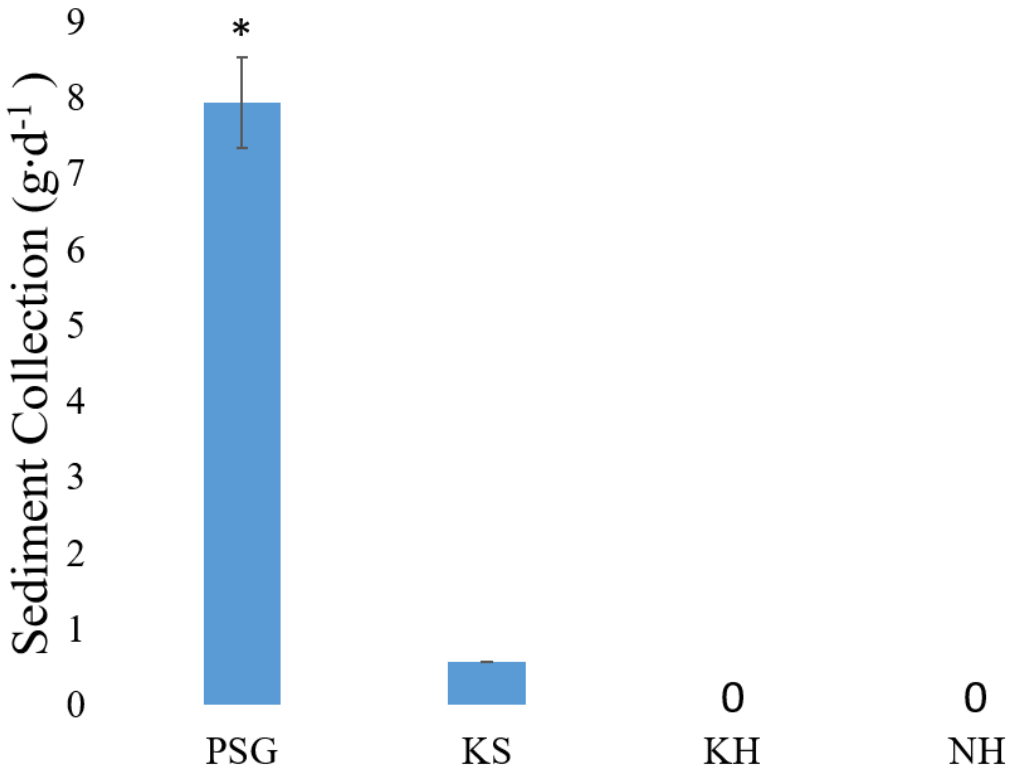

Figure 24. Mean (± SE) course sediment accumulation ($g \cdot d^{-1}$) in sediment traps at each representative habitat site (One way ANOVA $F_{3,6} = 121.6$, $P = 9.22x10^{-6}$). Site PSG was significantly higher in sediment than all other locations (Tukey's multiple comparisons of means: KS ($P = 4.04x10^{-5}$), KH ($P = 2.57x10^{-5}$), and NH ($P = 1.28x10^{-5}$)

APPENDIX C

Diet Richness and Proportion of *P. ochraceus* Prey Consumption

Diet Among Habitats shows sessile prey more commonly in bay and bench locations, but mobile prey was more commonly at boulder field habitats. Sea stars in the bay were only observed consuming barnacles (*Balanus glandula* and *Cthamalus dalli*; Fig 25) in the cardiac stomach; with consumption proportion of 0.11 (Fig 26). Boulder sites had lowest consumption proportion of 0.08 at PSG and moderate consumption of 0.14 at BB. I recorded the highest prey richness in sea stars in the boulder field sites (PSG and BB), with individuals observed consuming barnacles (*B. glandula* and *C. dalli*), black turban snails (*Tegula funebralis*), mussels (*Mytilus californianus*), and a chiton (*Lepitochitona*). Bench sites (KH and NH) had the highest proportion of sea stars consuming prey with 0.22 and 0.29, respectively. Prey consumption at both bench sites consisted primary of *M. californianus*, with one record of barnacles (*Semibalanus cariosus)* at KH.

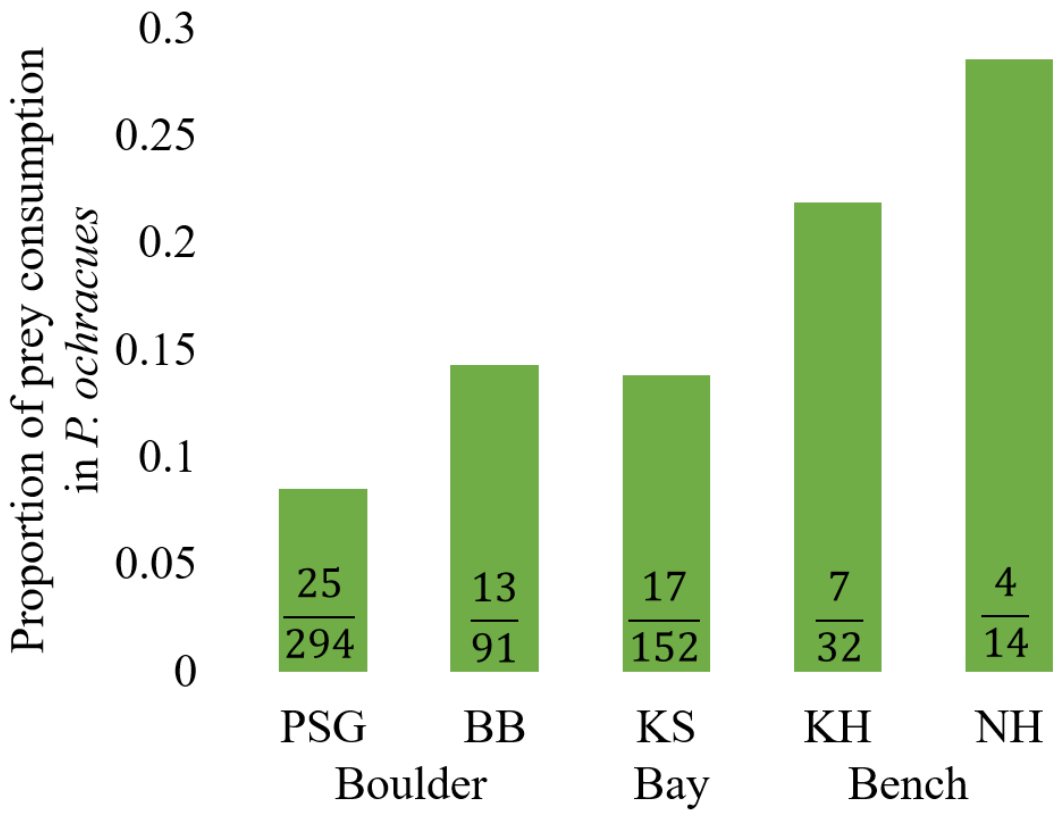

Figure 25. Proportion of prey consumption per site represented as a fraction on each bar. Key = Boulder Field Sites (PSG: Point St George, BB: Baker Beach), Bay (KS: King Salmon), Bench Sites (KH: Kibesillah Hill, and NH: Noyo Headlands).

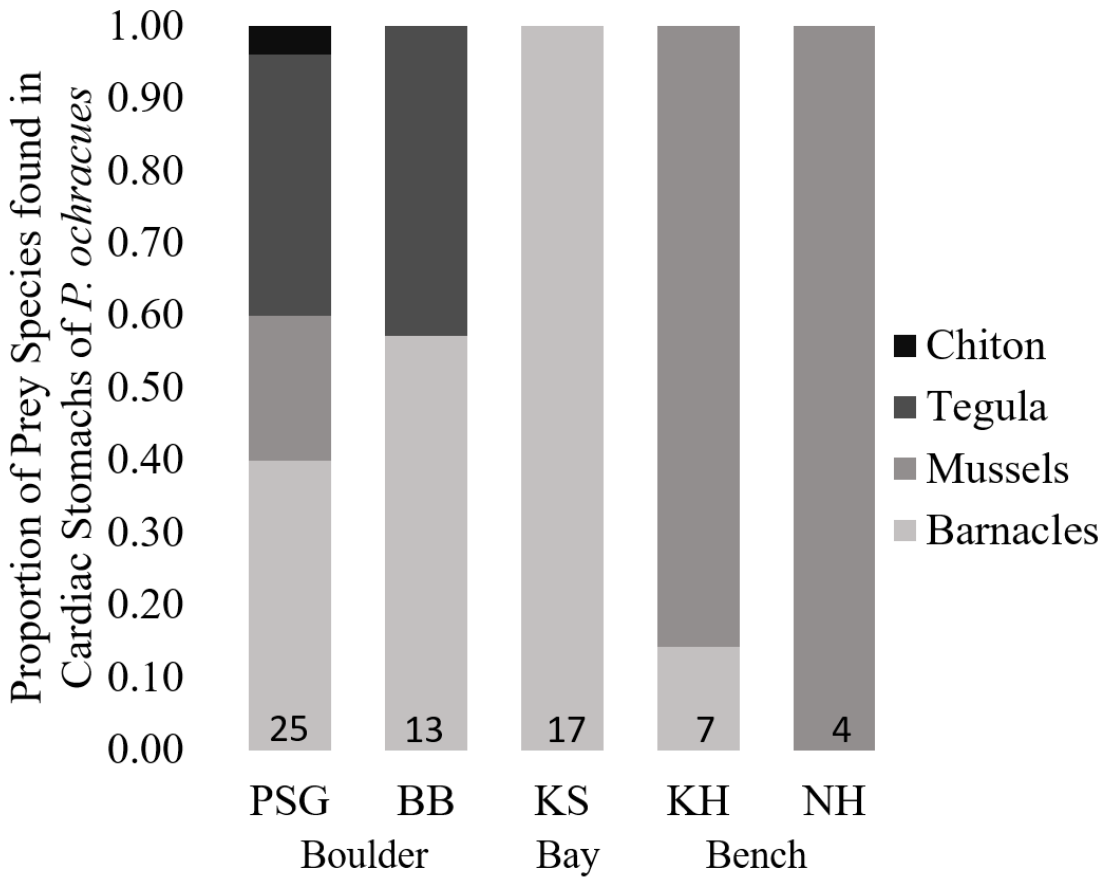

Figure 26. Proportion of compounding prey species found in *P. ochraceus'* cardiac stomach for each representative habitat site. Sample sizes of feeding *P. ochraceus* at each site are denoted at the bottom of each bar. Site initials as follows: Point St George (PSG), Baker Beach (BB), King Salmon (KS), Kibesillah Hill (KH), Noyo Headlands (NH).

APPENDIX D

Volumetric reconstruction of the skeletal portion of the aboral surface of two medium sized *P. ochraceus* using Micro CT scans from a large volume SkyScan 1173 desktop scanner at the Micro Photonics Imaging Laboratory in Allentown, PA.

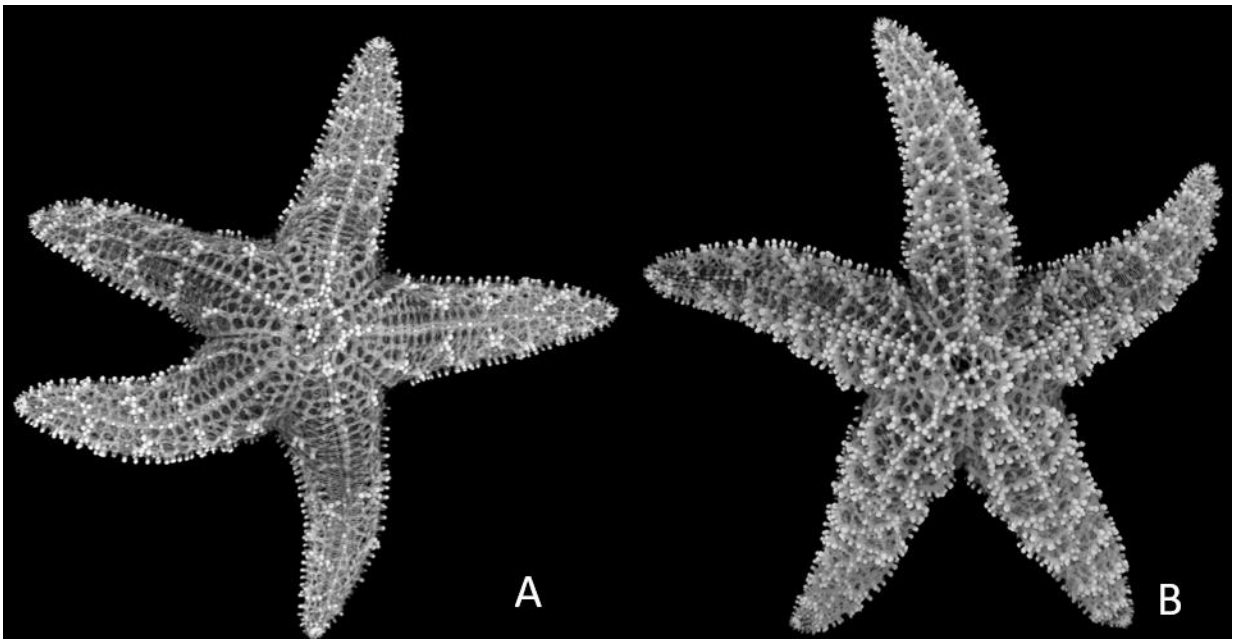

Figure 27. Volumetric reconstruction of the skeletons of two medium sized sea stars as a ‘nonspiny’ (A) and a ‘spiny’ (B) physical representation.